

A Critical Look at the Principles of Electromagnetic Time Reversal and its Consequences

**Walid Mohamed Galal Dyab¹, Tapan Kumar Sarkar¹, Alejandro García-Lampérez²,
Magdalena Salazar-Palma², and Miguel Angel Lagunas³**

¹Department of Electrical Engineering and Computer Science
Syracuse University

Syracuse, New York 13244-1240 USA

E-mail: wmdyab@syr.edu, tksarkar@syr.edu; <http://lcs.syr.edu/faculty/sarkar/>

²Departamento de Teoría de la Señal y Comunicaciones
Universidad Carlos III de Madrid

28911 Leganes – Madrid, Spain

E-mail: alamperez@tsc.uc3m.es, m.salazar-palma@ieee.org

³CTTC

Avda. Canal Olímpic, s/n 08860 Castelldefels, Barcelona, Spain

E-mail: m.a.lagunas@cttc.es

Abstract

A plethora of papers can be found in the scientific literature talking about time reversal. The term time reversal exists in the publications in a variety of different fields, such as ultrasonics, acoustics, wireless communications, electromagnetics, antennas and propagation, optics, physics, and philosophy. The term time reversal by itself sounds very interesting, and can provide many interpretations that are fascinating. However, due to a loose use of this term, it may in many cases lead to fallacious interpretations and conclusions if it is not interpreted in strict scientific terms. The main goal of this paper is to explain the appropriate definition of the term time reversal in electrical engineering in general, and in electromagnetics for wireless communications, to be specific. However, the motivation of the work presented in this paper is not to raise a controversy about time reversal and its related research. Rather, the aim of this work is to highlight the basic electrical-engineering fundamentals that are necessary to study time reversal and to correctly define it, and to then accordingly interpret the results. Hence, the true and fallacious benefits of electromagnetic time reversal will be exposed. To serve this purpose, the paper is divided into two parts. First, a detailed literature review is presented. The true history of the term time reversal in electrical engineering is traced. In this part, most of the reported definitions of time reversal and its claimed capabilities are summarized. Some problems with the application of time reversal in electromagnetics are discussed, both theoretically and practically. All of the time-reversal papers talk about reciprocal networks, so the fact of the non-reciprocity of a single-antenna system in the time domain (the way we generally interpret it) is presented, to prove theoretically that there is a problem with how we interpret time reversal in electromagnetics. Finally, practical examples are shown, where time reversal is used in a wireless system and in an acoustic de-reverberation problem. The exact capabilities of time reversal in electrical engineering are exposed in those experiments.

Keywords: Time reversal; electromagnetic time reversal; time reversal mirrors; time domain; impulse response; causality; channel impulse response; room impulse response; acoustic impulse response; inverse filtering; speech de-reverberation; biblade antennas; antenna reciprocity

1. Introduction

In the recent literature on wireless communications and Electromagnetics (from 2004 to the time of the writing of this paper), time reversal has been evolving as a new technology that provides solutions to wireless channel impairments in wideband wireless communications systems. There is a belief that the technology of time reversal has been successfully exploited in the ultrasonic domain since the early 1990s, and efforts are being exerted to exploit it in electromagnetics and wireless communications. To define what is meant by time reversal in this paper, and all of the considered references, we start with a simple example.

Imagine a situation where two players were throwing a ball to each other in front of a friend, who was recording them on a video camera. Player 1 first threw the ball to Player 2. Player 2 caught the ball and threw it again to Player 1. Player 2 was really careful to send the ball along the same direction he received it. When Player 1 was catching the ball, their friend who was recording them said that what he saw was exactly the same as the reversed movie of Player 1 throwing the ball. A debate started among them. They then decided to repeat everything again, but this time, Player 1 threw many balls in different directions. Player 2 received only the ball that came in his direction. Player 2 threw that ball again to Player 1. This time, their friend saw a totally different picture than what he saw on the reversed movie of Player 1 throwing the balls. The debate was over, and they concluded that what happened in the first case was a trick, and it was a successful trick because of several reasons. Some of the reasons were related to Player 2, and one reason was related to the medium in which they were playing. The five specific reasons were:

1. Player 2 received all that Player 1 threw.
2. Player 2 knew from which direction he received the ball.
3. Player 2 had the ability to throw the ball in the same direction he received it.
4. Player 2 did not change the shape of the ball either on receiving or on transmitting.
5. The medium allowed the ball to move in any direction, without any deformation.

If any of the above conditions do not hold, it is obvious that the trick will never be successful. In the context of the principle of time reversal, Player 2 is called a time-reversal mirror (TRM). Actually, what happened in the first case was that Player 2 (the time-reversal mirror) was cleverly able to imitate the reversed movie of Player 1 throwing the ball. However, for the second case, when Player 1 threw many balls in different directions, Player 2 was not able to imitate the reversed movie for Player 1 throwing the balls. It is obvious that if Player 2 in the second case is replaced by a team of players to collect all the balls thrown by Player 1 and send them back along the same

directions, only in this case will the team of players (the time-reversal mirror) be able to imitate the reversed movie.

Imagine repeating the same experiment using antennas and waves instead of players and balls. If we use one antenna instead of Player 2, the trick will never be successful. The antenna representing the time-reversal mirror in this case should be replaced by a huge number of antennas (team of players). This is important not only to be able to collect all waves sent from Antenna 1, but also to be able to resend them back along the same directions from which they were coming. Otherwise, the time-reversal mirror will never be able to imitate the reversed movie.

Now, let us consider the same example, but from a signal-processing point of view, using the basic fundamentals of linear time-invariant (LTI) systems.

Assume a linear time-invariant system with an impulse response, $h(t)$. The input is $x(t)$, and the output is $y(t)$. The output, $y(t)$, is given by

$$y(t) = x(t) \otimes h(t), \quad (1)$$

where \otimes denotes a convolution. Notice that conventionally, the system is considered to be excited from the left and is observed on the right, as shown in Figure 1. The same linear time-invariant system can be fed in the reverse direction, i.e., from the right to the left, without physically flipping the system. In this case, the impulse response of the system is $h_r(t)$. The input is $f(t)$, and the output is $g(t)$:

$$g(t) = f(t) \otimes h_r(t). \quad (2)$$

There are two conditions that have to be satisfied to claim that $h(t) = h_r(t)$. These two conditions are

1. The linear time-invariant system has to be reciprocal.
2. The output, $y(t)$, has to be defined as the reaction of the system to the input, $x(t)$. This means that if

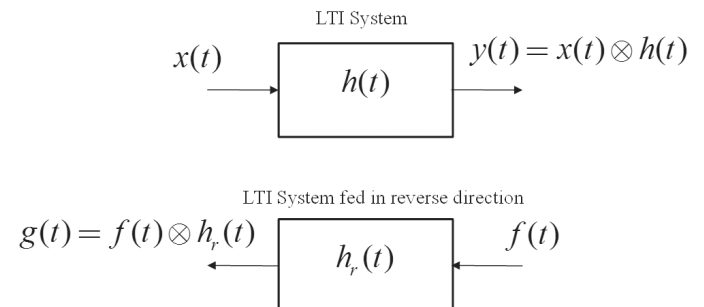


Figure 1. A block diagram of a linear time-invariant system fed from both sides.

the input signal is a voltage signal, the output has to represent a current signal, and vice versa. This is because reciprocity in electrical engineering applies to the product of *voltages and currents*, and not between *voltages and voltages*, such as for a transfer function!

Note that the second condition does not hold for the definitions of many electrical circuits' impulse responses, where the voltage gain is the quantity of interest in defining the circuit response. See Appendix 1 for more details on this condition.

If the system is reciprocal, then according to the reciprocity theorem of passive reciprocal networks, one can thus write

$$x(t) \otimes g(t) = y(t) \otimes f(t). \quad (3)$$

This means that if we apply the same input to either side of the system, we get the same output. In other words, if $f(t)$ is equal to $x(t)$, then $g(t)$ is exactly the same as $y(t)$.

To understand the time-reversal procedure, assume that the input, $x(t)$, is a Dirac delta function. The output, $y(t)$, is then by definition the impulse response, $h(t)$. Applying a time-reversal operator on the output, and feeding it back to the system with a reversed direction, Equation (2) becomes

$$g(t) = h(-t) \otimes h_r(t). \quad (4)$$

If $h(t) = h_r(t)$, then the output on the left-hand side, $g(t)$, by definition gives the autocorrelation function of the system impulse response, $h(t)$. That is,

$$g(t) = h(-t) \otimes h(t) = \int_{-\infty}^{\infty} h(\tau) h(\tau - T) d\tau = R_{hh}(t). \quad (5)$$

Equation (5) can be deduced from Equation (3) by the substitutions $x(t) = \delta(t)$, $y(t) = h(t)$, and $f(t) = h(-t)$. The output, $g(t)$, represented by the autocorrelation function $R_{hh}(t)$, is shown in Figure 2 for different impulse responses, $h(t)$. Note from Figure 2 that the effect of performing this procedure is to maximize the output, $g(t)$, at a specific instant of time. For example, if we look at the case shown in Figure 2f, the function $R_{hh}(t)$ looks similar to the excitation function, $\delta(t)$, but it can never approximate the function $\delta(t)$ because in the frequency domain, they are totally different functions. The time-reversal procedure is thus equivalent to a pulse-compression procedure acting on the impulse response, $h(t)$. Figure 2 illustrates the fact that the pulse-compression capability of time reversal (also known as temporal focusing) depends

mainly on the shape of the impulse response, and not on the procedure, itself. In other words, the ability of the time-reversal output, $g(t)$, to look like the exciting pulse, $\delta(t)$, depends mainly on the complexity of the function $h(t)$, and not on the time-reversal procedure itself. The more complex $h(t)$ is, the more compressed the output $g(t)$ is, and the more one can incorrectly claim that $g(t)$ is approximately equal to $\delta(t)$. This is why in all time-reversal papers, it is mentioned that temporal focusing of time reversal works better in complex inhomogeneous media than in simple media. This is simply because the impulse response of a complex inhomogeneous medium looks similar to the impulse response in Figure 2f, and its autocorrelation function looks (by illusion) more similar to a delta function. In fact, how well $R_{hh}(t)$ approximates a delta function depends mainly on the magnitude of the frequency response of $h(t)$, and not on its shape in the time domain. This fact is illustrated below.

Suppose that the input signal is any arbitrary signal $x(t)$. Applying the same procedure, the output will then be

$$g(t) = x(-t) \otimes h(-t) \otimes h(t) = x(-t) \otimes R_{hh}(t). \quad (6)$$

It is well known that for a causal impulse response, $h(t)$, the Fourier transform of which is $H(\omega)$, given by

$$\mathfrak{F}\{h(t)\} = H(\omega) = |H(\omega)| e^{-j\Theta(\omega)}, \quad (7)$$

the time-reversed signal, $h(-t)$, has a Fourier transform given by

$$\mathfrak{F}\{h(-t)\} = H^*(\omega) = |H(\omega)| e^{+j\Theta(\omega)}, \quad (8)$$

where $\mathfrak{F}\{\cdot\}$ denotes the Fourier transform, and the superscript $(*)$ denotes complex conjugation. $|H(\omega)|$ is the magnitude response of the linear time-invariant system $h(t)$, and $-\Theta(\omega)$ is its phase response. The Fourier transform of the autocorrelation function $R_{hh}(t)$ is given by

$$\mathfrak{F}\{R_{hh}(t)\} = \mathfrak{F}\{h(t) \otimes h(-t)\} = H(\omega) H^*(\omega) = |H(\omega)|^2 \quad (9)$$

Equation (9) clearly shows the contradiction between the need of $h(t)$ to represent a complex inhomogeneous medium (so that its autocorrelation is more compressed in time), and the need of $R_{hh}(t)$ to have a flat magnitude response (to represent a delta function).

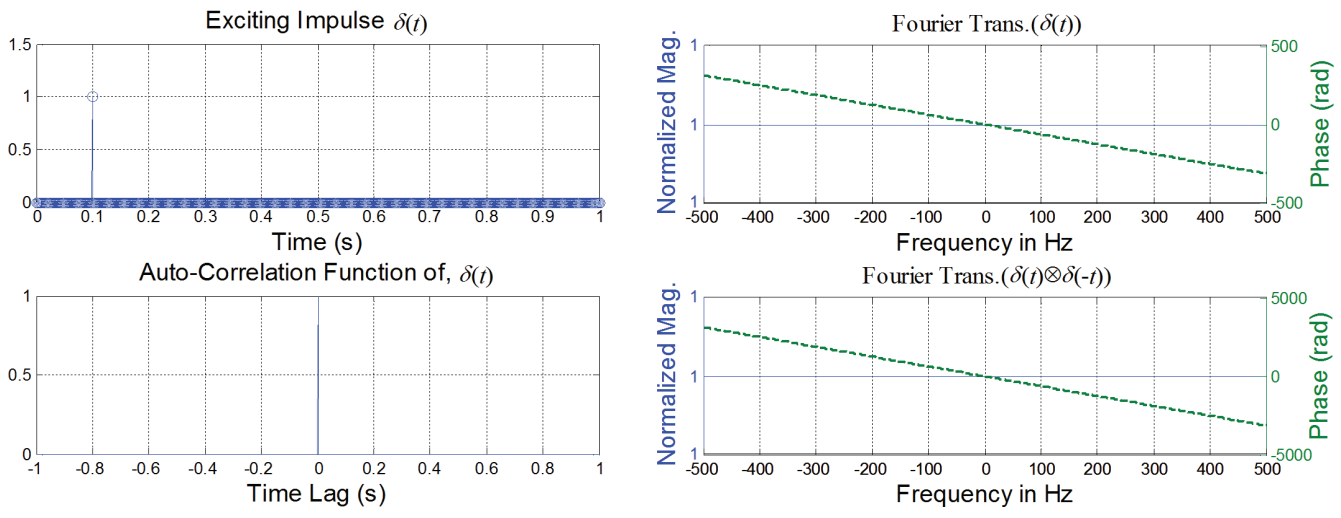


Figure 2a. The frequency response and autocorrelation properties of a pure impulse.

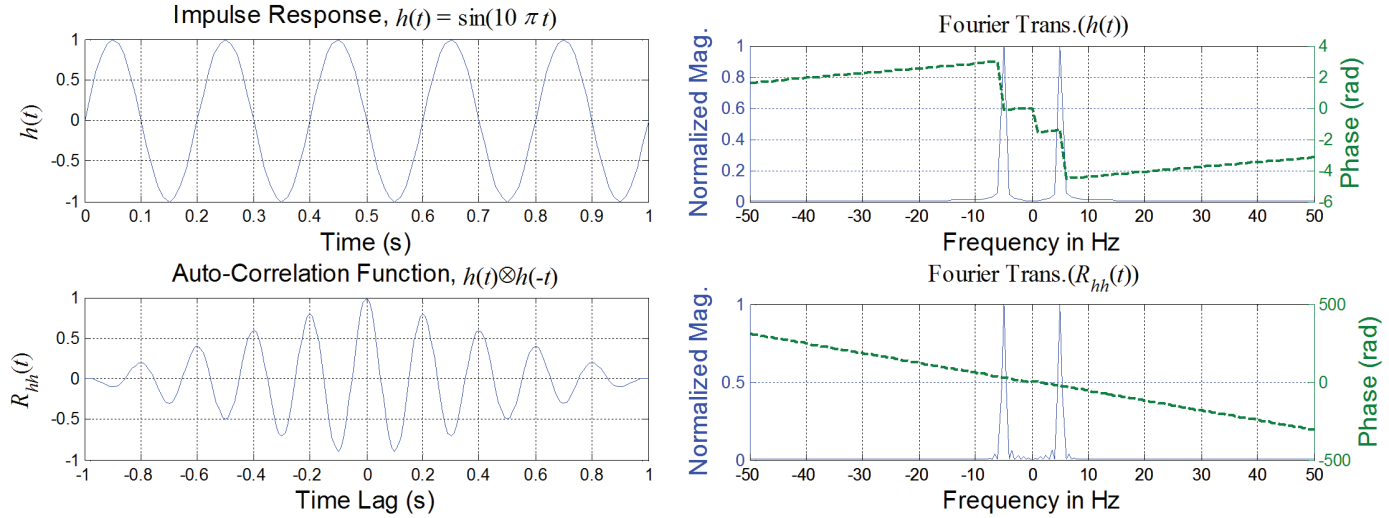


Figure 2b. The frequency response and autocorrelation properties of a sine function.

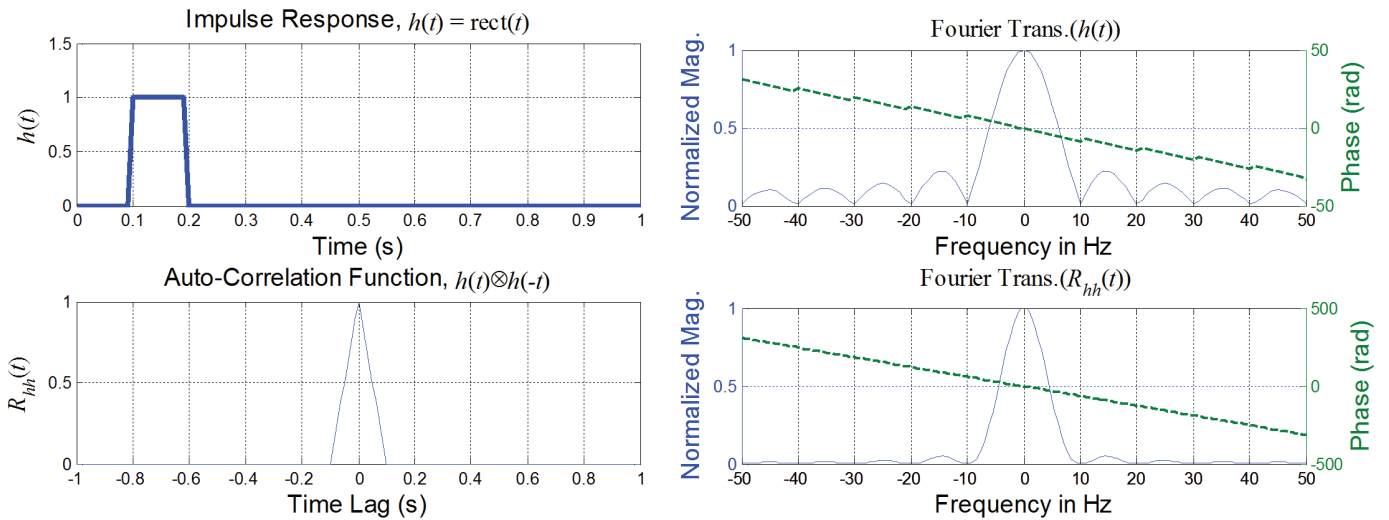


Figure 2c. The frequency response and autocorrelation properties of a rectangular function.

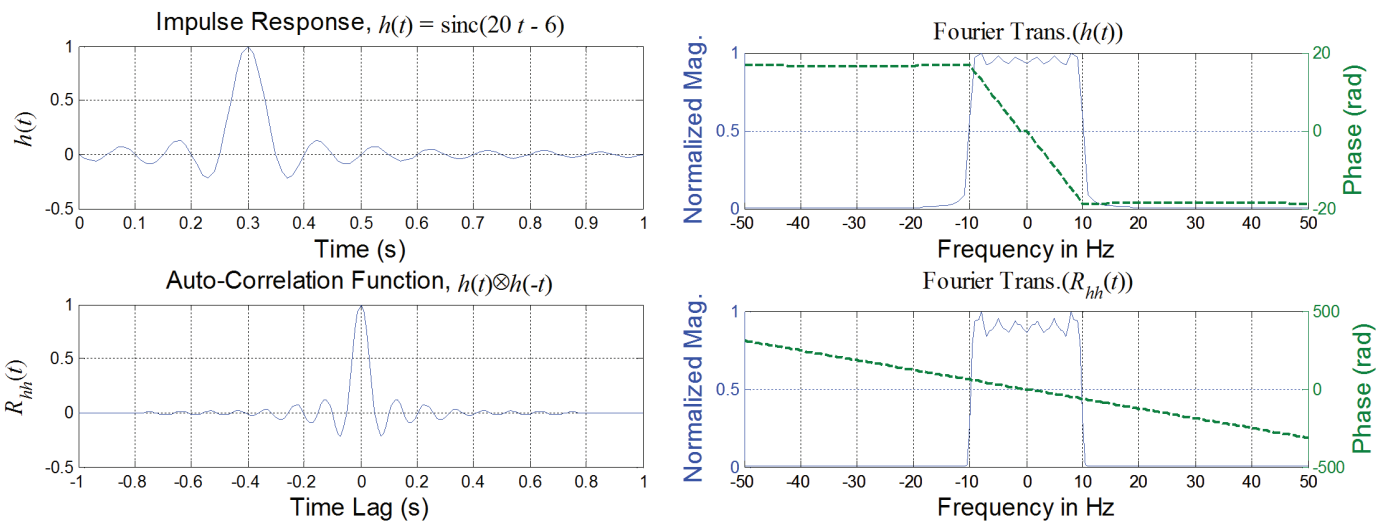


Figure 2d. The frequency response and autocorrelation properties of a Sinc function.

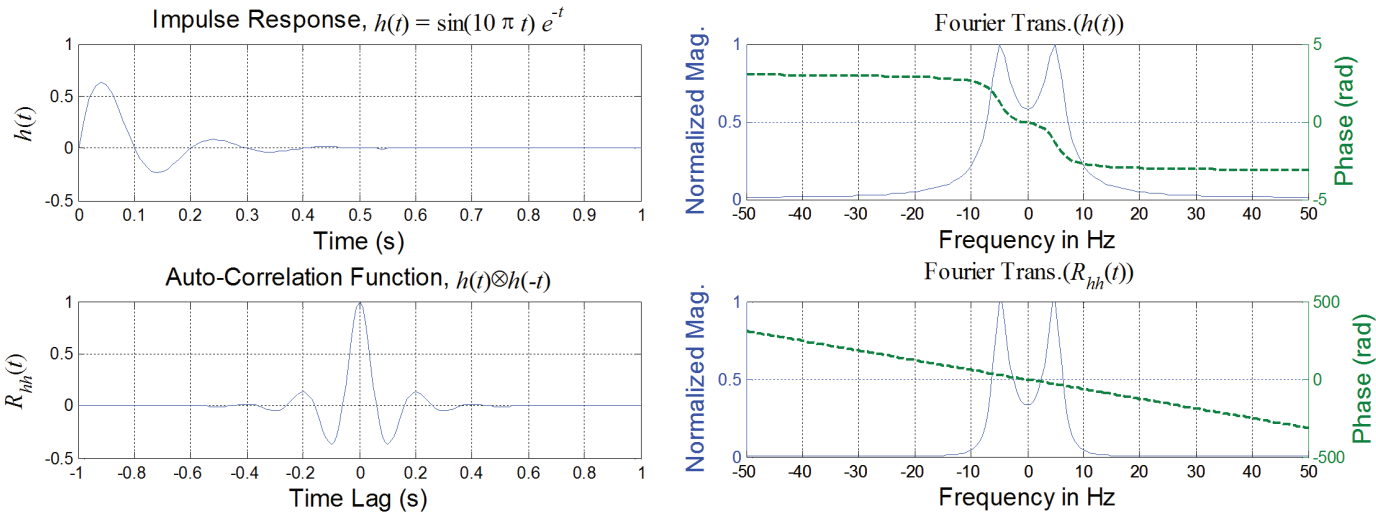


Figure 2e. The frequency response and autocorrelation properties of an exponential multiplied by a sine.

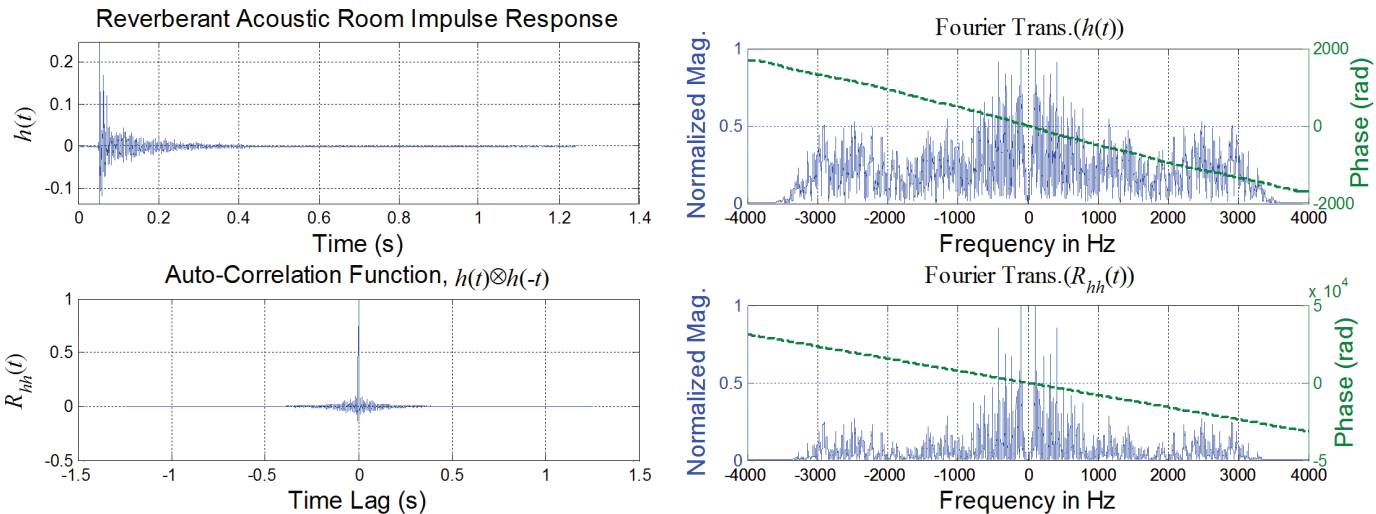


Figure 2f. The frequency response and autocorrelation properties of an actual reverberant acoustic room impulse response (RIR).

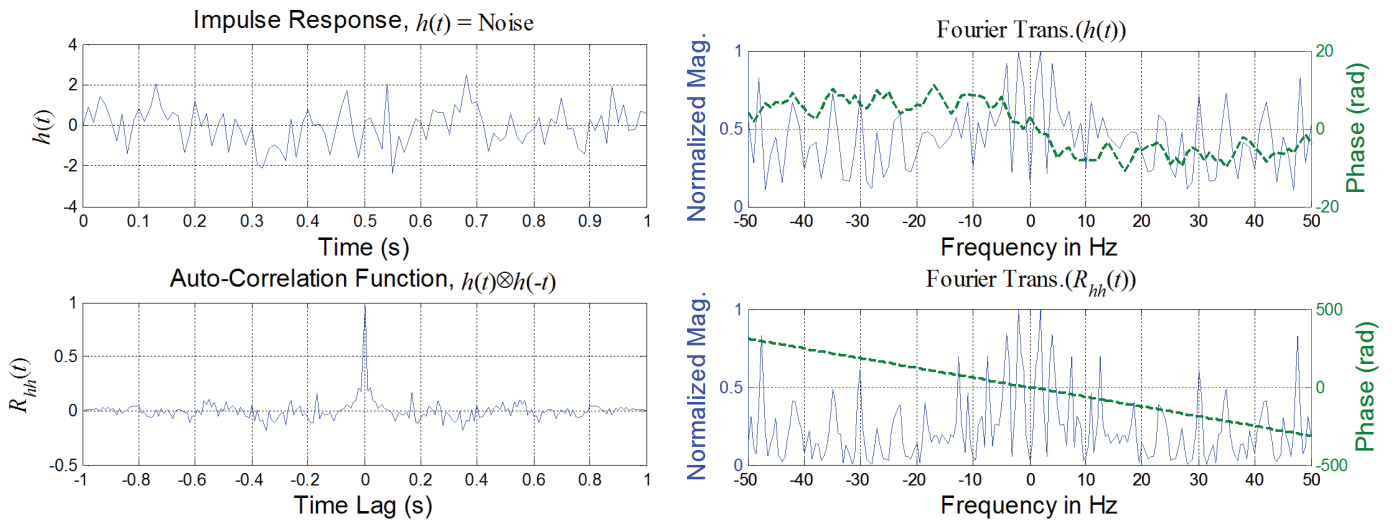


Figure 2g. The frequency response and autocorrelation properties of random noise.

We can now conclude from these fundamental principles of signals and systems that time reversal is defined as follows:

Given a reciprocal system,

1. Apply an input signal in the normal direction (left to right).
2. Get the reaction of the system to that input.
3. Flip the system's reaction in time (this can be done using a first-in last-out buffer).
4. Apply the flipped reaction as an *input*¹ to the system, but in reversed direction (right to left).
5. The observed reaction on the left side has the following characteristics:
 - a. It has a maximum value at a specific instant of time
 - b. It has the same phase as the input signal, but conjugated (i.e., with reversed sign). This means that the effect of the phase modification due to the system is eliminated.
 - c. The magnitude of its spectrum is the same as that of the input, but modified by the square of the magnitude response of the system.

Points (b) and (c) can be deduced by taking the Fourier transform of Equation (6):

¹This needs the conversion from current to voltage, or vice versa. See Appendix 1 for more details.

$$\mathfrak{F}\{g(t)\} = \mathfrak{F}\{x(-t) \otimes R_{hh}(t)\} = X^*(\omega) |H(\omega)|^2, \quad (10)$$

where $X(\omega)$ is the Fourier transform of the input signal, $x(t)$. It is obvious that applying the time-reversal procedure has one of the following effects:

- The first effect is to maximize the signal output at a certain instant of time. This is exactly what matched filters in many communications systems are used for. This is also the main idea of pulse-compression radars, where the signals are passed through matched filters to facilitate the detection of the existence of a certain waveform to which the filter is matched. It is well known that the impulse response of the matched filter is the time-flipped (or “time-reversed”) version of the signal to which it is matched. This effect cannot be achieved in time reversal unless the system is initially excited by an impulse. This effect is useful only for applications where the main goal is to detect whether or not the excitation impulse exists. Experiment 1 in this paper illustrates this concept.
- The other effect becomes apparent when the system is fed by a message signal, rather than an impulse. The effect of time reversal in this case is to compensate for the phase distortion of a dispersive system with a flat magnitude response. This is clear from Equation (10), where the input signal is modified by a zero phase function, which is $|H(\omega)|^2$. In other words, if the frequency response of the linear time-invariant system (which is $H(\omega) = |H(\omega)| e^{-j\Theta(\omega)}$) has a constant magnitude as a function of ω , then the effect of time reversal is just eliminating the phase distortion caused by

$\Theta(\omega)$. On the other hand, if the magnitude response is not constant with frequency, then time reversal still compensates for the phase distortion of the system, but at the same time makes the effect on the magnitude twice as worse. This will be clear in Experiment 2 in the last section of this paper.

Although most of the early papers on time reversal explicitly stated this conclusion, there exist many papers that take the advantage of time reversal out of its true context in a way that is very similar to the trick in the previously mentioned example of the balls. The aim in this paper is to clarify this subject, and to highlight the differences between the true and fallacious benefits of time reversal.

The rest of the paper is organized as follows. Section 2 gives a detailed literature review of the subject of time reversal. Throughout the literature review, the main goal is to track how time reversal evolved from just a signal-processing algorithm to a backward-propagation mechanism. Section 3 presents the theoretical fundamental challenges facing time reversal in wireless communications. This will be done by revisiting the reciprocity of antennas in the time domain. In Section 3, we conclude that the main challenge facing time reversal in wireless communications is the non-reciprocity of a single-antenna system, and that the high sampling frequency is not of much concern compared to that challenge. Section 4 shows two practical examples where time reversal is used in a wireless system, and also in an acoustic de-reverberation problem. The reason behind this choice is twofold. One, the application of the procedure in acoustics is quite straightforward and this will make the aspects of time reversal quite clear, since the system is not very sophisticated. Second, there is a belief that the procedure of time reversal started in acoustics. As will be clear from the literature review in the next section, there are efforts exerted now to apply it in wireless communications. It is thus interesting to see what time reversal can do in a reverberant acoustic problem, which is very analogous to the multipath problem in wireless communications. In Section 5, we conclude the paper. Finally, an appendix is added to discuss some important aspects of the reciprocity theorem, which is the basis of time-reversal technology.

2. Literature Review

To the best of our knowledge, the earliest paper in which the term “*time reversal*” was used – and defined in the same way as discussed in the introduction of this paper – was published in the year 1957 in the *IRE Transactions on Communications Systems* by B. P. Bogert of Bell Labs [1]. The paper demonstrated a time-reversal technique to compensate for the phase-delay distortion that appears on transmitting pictures and slow television signals on telephone lines. A block diagram of the technique presented in that paper is shown in Figure 3. The methodology was exactly the same as derived in Equations (1) -(9). Experiments were performed on data transmissions on a 5 KHz loop from Murray Hill, NJ, to Los Angeles, CA, and back. The data were received in Los Angeles, recorded, reversed in time, and retransmitted back to Murray Hill. Picture-quality enhancement was achieved by applying the same time-reversal procedure discussed in the previous section. The conclusion in that paper was, “These experiments demonstrate the ability of time-reversal techniques to correct the delay distortion of bisectable transmission circuits and networks. The improvement is most pronounced if the transmission characteristic of the system is uniform” [1]. It is interesting to note that one can come to the same conclusion by revisiting the time-reversal procedure from a signals-and-systems point of view, as we did in the previous section. A paper that was very similar to Bogert’s paper was published in the IBM journal in 1965 [2]. That paper dealt with the problem of automatic distortion correction for efficient pulse transmission over telephone networks. In the abstract of [2], it was explicitly mentioned that time-reversal systems compensate only for the distortion in the phase characteristic. The time-reversal procedure in [2] followed the same definition as in steps 1-5 in the introduction of this paper. It is important to note now that time reversal was a well-known technique in electrical engineering since the late 1950s. At that time, time reversal was used to compensate for phase distortions of linear systems. The same idea appeared in a paper in the *IEEE Transactions on Acoustics, Speech and Signal Processing* in 1974 [3]. In [3], the idea of time reversal was used to design digital filters with zero phase shifts. This idea was called “*noncausal digital filtering*.” Successive papers based on this type of filtering appeared in the literature during

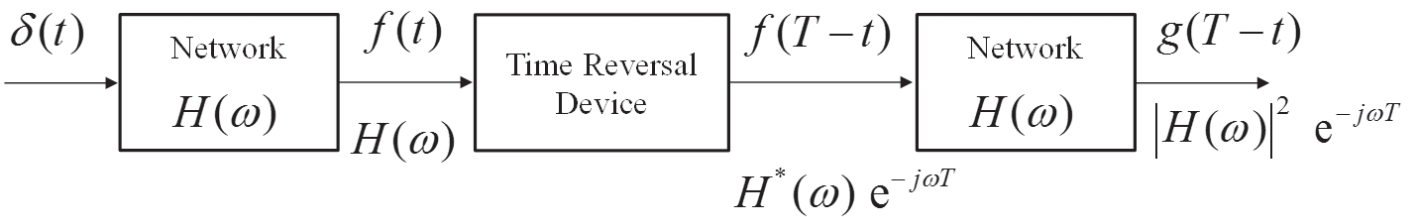


Figure 3. A block diagram of the experiment done by Bogert in [1]. The time delay, T , is dropped from the derivations here in this paper for the sake of simplicity.

the period 1982 to 1991 [4-7]. In [5], Daniel Harasty and Alan Oppenheim presented an approach based on noncausal filtering to solve the problem of *television-signal de-ghosting*. It is not of much importance here to know whether the approach they presented was successful or not. However, the important thing to note is that there were attempts – a long time ago – to use time reversal (inherent in noncausal filtering) to compensate for television-signal impairments due to multipath propagation. This is exactly what many researchers are currently trying to introduce in personal wireless communications. However, they have introduced it as a new technology that originated in acoustics in the early 1990s, and almost none of the recent papers gave any credit to the earlier work on time reversal, such as Bogert's work [1].

In 1992, a three-part paper appeared by Mathias Fink et al. in the *IEEE Transactions on Ultrasonics, Ferroelectrics, and Frequency Control* [9-11]. The paper was titled “Time Reversal of Ultrasonic Fields.” Fink's paper presented the time-reversal concept and time-reversal mirrors as new approaches for focusing ultrasonic fields. It is a fact that any researcher who starts working on time reversal (in general) will come to this paper and consider it as the foundation and basis of time-reversal technology (in general). Fink's paper [9-11] is highly appreciated. From studying Fink's work on time reversal [9-11], we find it important to make the following comments:

- The paper demonstrated time reversal in the context of the propagation of acoustic fields. This means that the block the impulse response of which is $h(t)$ in Figure 1 was now a channel in which the sound fields propagated. The two ports of the block represented the transducers on each side of the channel.
- The medium in which sound waves propagated was inhomogeneous.
- The time-reversal mirrors consisted of a transducer array of a large number of elements.
- The paper did not refer to the previous work on time reversal, such as [1-7].

Accordingly, one can conclude that in Fink's paper, the time-reversal mirror was a huge array that had a wideband spatial-processing capability. Basically, what Fink's time-reversal mirror did was that it received most of the propagated fields and retransmitted them along the same directions from which they were received. In Fink's paper, spatial focusing was thus involved, and not only temporal focusing. This is very similar to the example of the balls, where the time-reversal mirror consisted of a team of players to collect all the balls thrown by Player 1 and re-throwing all of them along the same directions. This analogy makes it clear that spatial focusing cannot be achieved except in one of the following cases:

1. The time-reversal mirror is built of a sensor array that can apply wideband spatial processing on

receiving and on transmitting. This is exactly what Fink's time-reversal mirror in [9] represented. It is only by chance that the procedure of acoustic wideband beamforming is exactly the same as the procedure of time reversal. In Fink's paper, 64 transducers were used as the time-reversal mirror. The 64 transducers recorded the incident fields. In the next step, the time-reversed fields were then re-emitted from all the transducers. This is exactly the same procedure of wideband beamforming that depends on time delays rather than phase shifts.

2. The medium itself confines all of the transmitted energy towards the time-reversal mirror: by the reciprocity of the medium, any waveform transmitted by the time-reversal mirror will thus be confined to the source location. This case resembles a simple waveguide with more than one mode propagating. Spatial focusing appears between the two ports of the waveguide regardless of the waveforms, i.e., spatial focusing appears due to the medium, not due to time reversal.
3. Case 2 can be explained in a different way. In a time-reversal procedure, assume that the pulse, after being reversed and retransmitted, is being received at a location other than the original source. Let the impulse response from the time-reversal mirror to that location be $h_2(t)$. Equation (5) then becomes

$$g_2(t) = h(-t) \otimes h_2(t) = R_{hh_2}(t) \quad (11)$$

and we then hope that this function is minimum for all values of time. In other words, the claimed spatial focusing of time reversal assumes a very low cross correlation between $h(t)$ (the impulse response from the time-reversal mirror to the source) and $h_2(t)$ (the impulse response from the time-reversal mirror to any other location). Unfortunately, this strongly depends on the environment, and there is no available means to control it. The cross-correlation properties of some channel impulse responses are shown in the last section of this paper.

Twelve years after his famous paper [9-11], Fink coauthored some papers presenting time reversal of electromagnetic waves [14, 15]. In [14], it was said that, “...we present the first one channel electromagnetic time reversal mirror working around 2.45 GHz.” The conclusion in [14] mentioned the successful temporal and spatial focusing of a single-channel time reversal. It is important at this point to show a block diagram of the experiment that was carried out. Figure 4 shows a block diagram of the experiment presented in [14]. The experiment was performed in a closed reverberant chamber. One antenna was considered as the source, which sent a modulated carrier to the time-reversal mirror. The time-reversal mirror, which was a single receiving antenna, applies phase conjugation of the carrier and the modulating signal, and retransmitted them

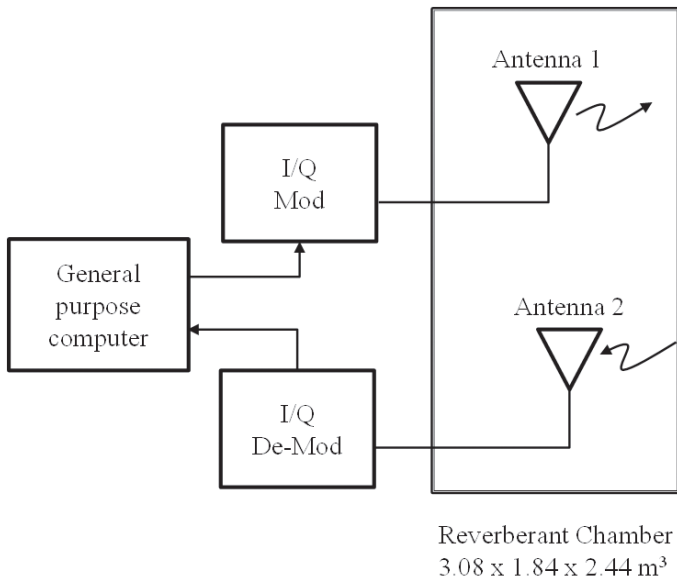


Figure 4. The experiment presented in [14], where it was said to be the first electromagnetic time-reversal experiment.

back to the source. In the results of the paper, the claimed spatial focusing was justified by showing the field strength at the source and at locations away from the source after applying time reversal. The results showed high field strength at the source, and low fields at other locations several wavelengths away from the source. The field strengths at the other locations was not compared before and after applying time reversal. This comparison might have shown whether the spatial focusing was related to the time-reversal procedure, or if it solely depended on the propagation medium, which was a reverberant chamber. Actually, it was stated in [14] that “since we have only one-channel time reversal, no focusing would occur in free space no matter how large the bandwidth is; in a reverberating medium no focusing would occur either if the bandwidth is too narrow.” This fact was not conveyed to later work in the same field by other researchers. For example, in [16], time reversal using one-by-one antennas was presented, and spatial focusing was said to be achieved, which contradicted what was concluded in [14]. Also in [16], the spatial field distribution was not shown before applying time reversal. In [17], a definition that enforced that time reversal had a spatial-focusing capability inherent in it was given. It was said in the introduction of [17]:

In a time reversal (TR) experiment, a transducer captures the response received from an impulsive point source, and re-emits the time reversed version of this response into the propagation medium. For nondissipative media, the emitted signal back-propagates and focuses in both **space and time** at the original impulsive source....For richly scattering media, this space time compression can be very strong.

This paragraph [emphasis added] provided an indefinite conclusion, because it lent the spatial and temporal focusing

characteristics to the time-reversal procedure, and not to the propagation medium. What it only said about the propagation medium was that a richly scattering medium caused a stronger focusing. Furthermore, it was concluded in [17] that time reversal should lead to improved wireless communication systems by high reliable transmission and reduced interference to co-channel users. That is where we believe that time reversal started to be viewed as a backward-propagation mechanism. This view starts by giving the time-reversal procedure all the credit for spatial and temporal focusing, without considering either the medium or the structure of the time-reversal mirror, itself. Concentrating on the spatial and temporal focusing of time reversal took the subject little by little out of the context of matched filtering, and put it in the shape that time reversal really reverses the mechanism of propagation of the field inside the medium. For example, this claim was explicitly stated in a paper that appeared in the *IEEE Antennas and Propagation Magazine* in 2010 as follows: “The time reversal electromagnetic chamber basically exploits the properties of time reversal by ideally reversing the time evolution of a field distribution originally generated by a given source of radiation” [13]. In a different paper, the following definition for time reversal is given: “The principle of time reversal is to let acoustic or electromagnetic waves live backward their propagation in a complex environment to focus back to the initial point of their generation” [34].

It is clear that there are two views of time reversal that are mixed together. One view deals with the subject as a signal-processing technique, which has some useful effects in some situations. This view was presented mainly in the work of Bogert and his followers during the period from the late 1950s to the early 1990s. The other view defines time reversal as the backward propagation of the waves converging back to their source. The later view started roughly in 2004, and dominates the current work on time reversal. In order to help the interested reader in following our analysis in this literature review, we categorize most of the available papers in which time reversal is applied to electromagnetics into four categories, as follows.

2.1 First Category

This includes papers by Fink, starting from his famous and interesting papers in the late 1990s on ultrasonics [9-11, 18], passing by his 2004 paper that reinitiated the work on time reversal in electromagnetics [14], and ending with his 2010 paper in the *IEEE Transactions on Antennas and Propagation* on the theory of the electromagnetic time-reversal mirror [12]. A detailed explanation for [12] is given in the next section.

2.2 Second Category

This category includes papers applying time reversal to the problem of multipath wireless communications. These can be found in [17, 19-28]. In all of those papers, it was clearly stated that the main aim of the work was to apply the success-

ful experiments of Fink on time reversal to the field of wireless communications. Time reversal was introduced in this category as a promising technology to solve the impairments caused by multipath fading. This was justified by the previously mentioned spatial and temporal focusing capabilities of time reversal. To show the great influence that the papers of the first category had on the papers of the second category, we mention the following interesting observations:

1. In [18], it was shown that analog-to-digital conversion, using only one-bit representation, was enough to apply time reversal. This meant that when sensing the impulse response, it was enough to sense the sign of the signal to apply time reversal, i.e.,

$$R_{hh}(t) \approx \hat{R}_{hh}(t) = h(t) \otimes \text{sign}\{h(-t)\} \quad (12)$$

where

$$\text{sign}\{h(t)\} = \begin{cases} +1 & \text{if } h(t) > 0 \\ -1 & \text{if } h(t) < 0 \end{cases}$$

In [22], the same thing was applied with a title “One-Bit Time Reversal for WLAN Applications.” Although the work presented in [22] was appreciated, there was a little confusion that this title might cause when it said “One-Bit for WLAN” instead of “One Quantization-Bit Time Reversal for WLAN.” This little confusion represented one of the motives for highlighting the challenges that might appear when time reversal, presented in ultrasonic experiments [9], is extended to electromagnetics and wireless applications.

2. Since the high frequencies needed to digitize microwave signals is a real problem facing the application of time reversal in electromagnetics, the experiment involving time reversal in [14] was therefore carried out on a monochromatic wave. This workaround was done in all of the experimental tests that followed [14]. This was the only reason that explains why in [19-21, 23-25, 27] the autocorrelation function, $R_{hh}(t)$, was defined as

$$R_{hh}(t) = h(t) \otimes h^*(-t) \quad (13)$$

where the superscript $(*)$ denotes complex conjugation. It is well known that $h(t)$ represents a physical channel, and it is always a real function of time. The superscript $(*)$ should appear only in the frequency domain, as shown in Equation (8), even if harmonic time variations ($e^{j\omega t}$) are considered.

The last paper in this category proposed a new wireless technology based on time-reversal-division multiplexing [28]. In brief, this meant that in a cellular system, for example, the

channel impulse responses from the base station to each individual user could be used as a group of orthogonal waveforms, instead of the conventional pseudorandom codes. If this is the case, then it is necessary to study the autocorrelation and cross-correlation properties of those impulse responses. This is done in experiment 1 in this paper.

2.3 Third Category

Time-reversal ultra-wideband communications in indoor and reverberant environments were presented in this third category of papers, along with time-reversal electromagnetic chambers [13, 29-40]. The reason we put these papers into one category was because all of them were published by research groups from French universities and labs. It seems that Fink’s work, also initiated in France, had a great influence on many research groups. All of the references [13, 29-40] thus showed applications of time reversal in different systems based on the same time-reversal concepts presented in the first category of papers. The spatial-focusing capability for time reversal was not clearly justified in those papers. On the other hand, it was concluded in [29] that “for standard indoor channels we observe a TR gain collapse. Time reversal in those cases may not be as effective as expected in [14].”

2.4 Fourth Category

The last category includes most of the work applying time reversal to radar and imaging problems, such as [41-50]. This type of work mainly depended on the pulse-compression capabilities of time reversal to detect targets in densely cluttered environments. There is a great analogy between the work presented in those references and the pulse-compression techniques applied by matched filters in conventional radars. However, the main limitation facing those techniques was the necessity of the deconvolution of the detector responses. For example, in [50], where the idea of object imaging using time reversal of terahertz pulses was proposed, it was clearly stated that the response of the terahertz pulse detector limited the image-reconstruction procedure: “Clearly, we are able to determine a basic outline of the object, but because of the convolution of the THz waveforms with the detector response, we are not able to completely resolve this object” [50]. This means that antenna responses in time-domain electromagnetics are some of the major concerns that have to be thoroughly studied before applying any new wireless technology based on time reversal. The next section presents this issue in more detail.

3. Electromagnetic Reciprocity

From the discussion given in the literature review, the real history of time-reversal in electrical engineering is now clear. The two mixed views of time reversal have been highlighted,

and most of the papers available in the literature about time reversal have been categorized according to their perspectives. The remaining goal in this paper is to show the inapplicability of one of these views, namely the definition of time reversal as a back-propagation mechanism that attracts the waves back to their sources. The practicality of the other view is then discussed, namely the definition of time reversal as a normal signal-processing algorithm, which has no relationship to the back-propagation mechanism of waves. This is done through a theoretical discussion of electromagnetic reciprocity, and practical experiments on wireless as well as acoustic systems.

We first consider the paper published in 2010 in the *IEEE Transactions on Antennas and Propagation* with the title, “*Theory of Electromagnetic Time-Reversal Mirrors*” [12]. The paper talked about the time symmetry of Maxwell’s equations, the use of a six-vector formulation for the integral equation of time reversal, and defined a 6×6 Green’s function. As stated in the conclusion in [12], using an integral approach, a general expression for time reversal was then been obtained that is always valid. The work presented in the paper to put forth a theory for time reversal in electromagnetics is highly appreciated. However, due to the importance of the subject, we attempt in this paper to add some factors that we believe are very important.

Time reversal is defined in [12] as follows: “A time reversal mirror is a device that produces an outgoing wave which is the time-symmetric of an incoming-wave.” This means that if the original source sends an impulse to the time-reversal mirror, the time-reversal mirror should respond with a signal that looks at the original source exactly as the exciting impulse. According to this definition, time reversal is thus related to inverse filtering. The inverse of a certain linear time-invariant system is the filter that estimates the input of the linear time-invariant system from its output. The last experiment we present in this paper shows more details of the relationship between time reversal and inverse filtering.

To avoid the practical difficulty of digitizing signals in the GHz regime, the theory of time-reversal mirrors given in [12] is derived for monochromatic waves. This means replacing time reversal with phase conjugation. According to the definition in the previous point, the original source should send a sinusoidal waveform to the time-reversal mirror; then after time reversal, the signal received from the time-reversal mirror at the original source should be exactly as the initial signal, i.e., sinusoidal. Since sinusoidal signals are the eigenfunctions of the time-derivative operator that relates the temporal behavior of the inputs and outputs of all electrical systems, the output of the time-reversal system is therefore expected to be sinusoidal of the same frequency as the input, except for a phase and amplitude modification. This will be the case whether or not time reversal is applied. In other words, monochromatic signals cannot be used to study or appreciate the characteristics of time-reversal systems.

The perfect time-reversal mirror discussed in [12] is composed of a large number of antennas surrounding the original

source. According to [12], in order to completely reverse the propagation mechanism, all of the fields transmitted by the original source should be collected and re-transmitted back in a reversed order. If the reader remembers the example of the balls, this is very similar to use a team of players (instead of Player 2) to collect all of the balls thrown by Player 1. In fact, the time-reversal mirror that collects all the fields transmitted from the original source, as shown in [12], is impractical to implement.

The derivation in [12] used the reciprocal characteristics of the medium as the main enabling feature of back propagation. Specifically, Hermitian permeability and permittivity tensors were assumed: otherwise, the time-reversal derivations do not work. The important issue that needs to be discussed here as well is the reciprocity of the transducers (antennas, in electromagnetics). Actually, reciprocity relations of antennas are not as straight forward as the reciprocity relations of the acoustic transducers may be. In the following subsection, the reciprocity relations of antennas in the time domain are discussed.

3.1 Single Antenna Reciprocity

It is clear that reciprocity is the main key enabling time reversal in any kind of channel. For wireless channels, antennas are the only kind of transducers used to convert from currents and voltages to electric and magnetic fields, and vice versa. If one tries to prove the reciprocity of antennas for time-harmonic excitations – namely, proving that the receiving and transmitting antenna patterns are identical – one will end up getting the universal equation

$$A(\theta, \varphi) = \frac{\lambda^2}{4\pi} G(\theta, \varphi), \quad (14)$$

where λ is the wavelength associated with the radial frequency ω . $A(\theta, \varphi)$ is the effective area of the antenna, and represents its receiving power pattern. $G(\theta, \varphi)$ is the gain of the antenna, and represents its transmitting power pattern. Equation (14) is universal in the sense that it is valid for any type of antenna. A detailed proof for Equation (14) can be found in [52]. It can be inferred from Equation (14) that the receiving and transmitting power patterns of the antennas are identical, except for a multiplicative constant. The fact that is often missed and ignored is that Equation (14) directly tells us that the receiving and transmitting patterns in the time domain are not identical. To see this fact, first take the square root of Equation (14), and substitute $2\pi c/\omega$ for λ , where c is the speed of the wave in the medium. Equation (14) becomes

$$a_t(\omega, \theta, \varphi) = \omega \frac{1}{c\sqrt{\pi}} a_r(\omega, \theta, \varphi), \quad (15)$$

where $a_t(\omega, \theta, \varphi)$ is the transmitting field pattern and

$a_r(\omega, \theta, \varphi)$ is the receiving field pattern of the same antenna. Taking the inverse Fourier transform of Equation (15) gives the relationship between the transmitting and receiving field patterns in the time domain. From Equation (15), it is clear that the function relating the transmitting and receiving patterns of the antenna in the frequency domain is a linear function in ω . The relationship in the time domain is thus through a time-derivative operator, i.e.,

$$\begin{aligned}\mathfrak{F}^{-1}\{a_t(\omega, \theta, \varphi)\} &= \frac{d}{dt}\mathfrak{F}^{-1}\left\{\frac{1}{jc\sqrt{\pi}}a_r(\omega, \theta, \varphi)\right\} \\ \Rightarrow a_t(t, \theta, \varphi) &\propto \frac{d}{dt}a_r(t, \theta, \varphi).\end{aligned}\quad (16)$$

In the time domain, the transmitting field pattern of the antenna is the time derivative of the receiving field pattern of the same antenna. The same conclusion can be reached following a detailed derivation that was given by Glenn Smith in [51]. The final expression of a single-antenna reciprocity theorem in the time domain in [51] is given by

$$V_r^-(t) \otimes \frac{dI_t^+(t)}{dt} = \frac{2\pi}{\mu_0} \bar{E}^i(0, t) \otimes r\bar{E}^t(-r\hat{k}_i, t + r/c), \quad (17)$$

where μ_0 is the permeability of the medium. The expression of Equation (17) can be very easily explained based on the simple understanding of the reciprocity theorem. The configuration of the single antenna shown in Figure 5 can be considered as a two-port network. One of the ports is a lumped port that represents the feeding port of the antenna, whereas the other port is a distributed port, representing the fields on an imaginary surface, S , surrounding the antenna. On transmitting, the

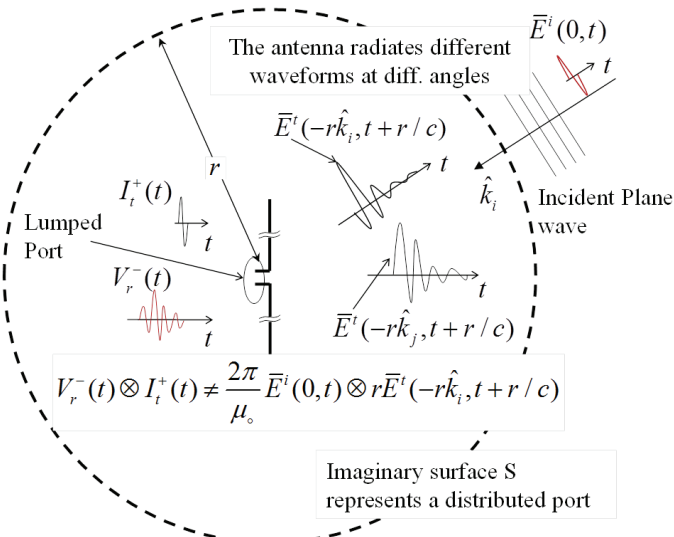


Figure 5. Single-antenna non-reciprocity.

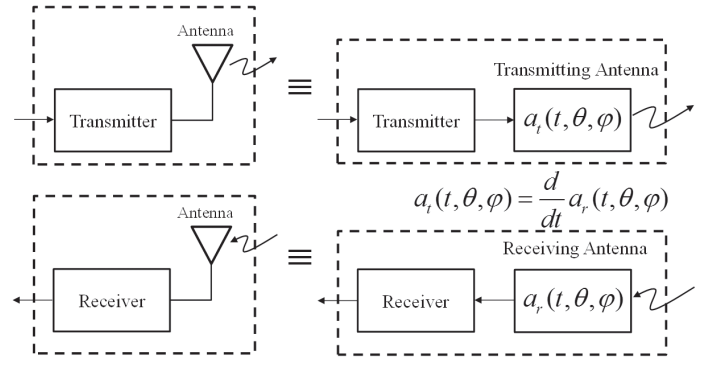


Figure 6. A block diagram of the same antenna when it is used as a transmitter (upper part) and as a receiver (lower part).

antenna is fed by a current $I_t^+(t)$. The reaction on the surface S due to $I_t^+(t)$ is an electric field given by $\bar{E}^t(-r\hat{k}_i, t + r/c)$, where r is the radius of the enclosed sphere S , and \hat{k}_i is a unit vector in the direction of propagation of the incident wave when the antenna is receiving, as shown in Figure 5. On receiving, a magnetic field $\bar{H}^i(0, t)$ (that can be easily related to the incident electric field $\bar{E}^i(0, t)$ in Equation (17)) is applied to the distributed port S , and the reaction to this incident field at the lumped port is an open-circuit voltage, $V_r^-(t)$. If the single-antenna system is reciprocal, one should expect that Equation (17) should be written as follows:

$$V_r^-(t) \otimes I_t^+(t) \propto \frac{1}{\eta_0} \bar{E}^i(0, t) \otimes \bar{E}^t(-r\hat{k}_i, t + r/c), \quad (18)$$

where η_0 is the intrinsic impedance of the medium. Equation (18) means that the transmitting current convolved with the open-circuit voltage on receiving is proportional to the field on S due to the transmitting current convolved with the incident magnetic field applied on S when the antenna is receiving. Unfortunately, this is not the case, and Equation (18) is not correct. Equation (17) is what we get following either a detailed derivation, as in [51], or using a simple procedure as we get in Equation (16). We therefore must conclude from this that a single-antenna system is not reciprocal, at least in the conventional sense of reciprocity. Actually, if an antenna is fed by an impulsive current, it radiates along a given direction an electric field as a certain function of time. This function is exactly the time derivative of the open-circuit voltage measured at the antenna's terminals when an impulsive electric field is incident on it from the same direction. This fact was shown by simulations and measurements in [53]. Accordingly, the block diagram for a transmitting antenna in an electrical system must not be the same as the block diagram for a receiving antenna, even if the antennas are identical. Figure 6 illustrates this fact. In the frequency domain, the problem does not exist, because the antenna's responses are within a multiplicative constant. This is again because harmonic excitations are the eigenfunctions

of linear electrical systems. A sine wave times a complex constant is still a sine wave, but with different amplitude and phase; however, the frequency is never changed in a linear system, which is the case with Maxwell's equations in linear media. If an antenna is fed by any arbitrary function of time other than the harmonic functions, the radiated field is thus certainly a different function of time. The radiated field is determined by the antenna's shape and the direction along which the field is observed. Furthermore, this mechanism is not reversible, since a single-antenna system is not reciprocal, as shown in Figure 5. The important question is now, how would time reversal work if viewed as a back-propagation mechanism? The answer is there is no way, because the reciprocity of the medium, which is the main key of the claim of the back-propagation mechanism, does not hold for antennas. Additionally, this fact was stated clearly in [50], where the detector's response was the main limitation facing the process of object reconstruction in Terahertz imaging using time reversal.

However, in fact single-antenna systems are not found, in practice. In any wireless system, there will be at least two antennas – one transmitting and the other, receiving. Even if the receiving antenna is a simple probe, it is still an antenna. From practice, we know that a two-antenna system is reciprocal, so the question is, how is a two-antenna system reciprocal, while a single-antenna system is not?

3.2 Two-Antenna Reciprocity

The discussion given in the last subsection is very important for highlighting the fact that it is often wrongly assumed that a single antenna, by itself, is reciprocal, since a full wireless system is. This issue is clarified by explaining why a two-antenna system is reciprocal.

Assume a two-antenna wireless channel: one antenna is transmitting, and the other is receiving. The complete block diagram of the two-antenna channel is shown in Figure 7. The impulse response of the whole system, fed from left to right, is given as

$$h_{left-right}(t) = a_t^1(t) \otimes h(t) \otimes a_r^2(t) \\ = \left\{ \frac{d}{dt} a^1(t) \right\} \otimes h(t) \otimes a^2(t), \quad (19)$$

whereas the impulse response of the system fed right to left is given by

$$h_{right-left}(t) = a_r^1(t) \otimes h_r(t) \otimes a_t^2(t) \\ = a^1(t) \otimes h(t) \otimes \left\{ \frac{d}{dt} a^2(t) \right\}, \quad (20)$$

where

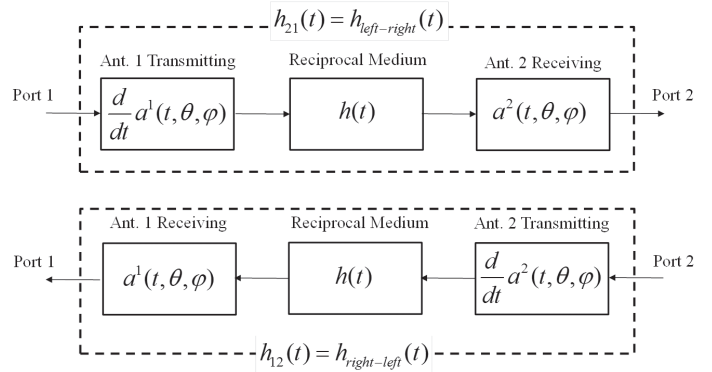


Figure 7. Two-antenna-system reciprocity.

$$\begin{cases} a_r^i(t, \theta, \varphi) = a^i(t, \theta, \varphi) \\ a_t^i(t, \theta, \varphi) = \frac{d}{dt} a^i(t, \theta, \varphi) \end{cases} \text{ for } i = 1, 2, \quad (21)$$

and the arguments θ and φ have been dropped in Equations (19) and (20) for simplicity. Given a reciprocal medium ($h(t) = h_r(t)$), it is clear that Equations (19) and (20) are identical if the location of the time-derivative operator can be interchanged. It is also clear that Equations (19) and (20) are exactly identical in the frequency domain. The conclusion is thus that a single antenna is not reciprocal, because its impulse response on transmitting is not equal to its impulse response on receiving. However, the transmitting and receiving impulse responses are not totally independent: they are related through a time-derivative operator. In addition, since the transmitting and receiving impulse responses of the two antennas are related through the same relation, the two-antenna system is therefore reciprocal despite the fact that a single-antenna system is not. Hence, time reversal in electromagnetics should be considered as a signal-processing algorithm, concerned only with terminal-to-terminal signals, using Equations (19) and (20). Looking into the field propagation mechanism and considering time reversal to reverse the propagation in time is a completely wrong approach that is invalid in electromagnetics. In acoustics, where the fields are scalar and not vector fields as in electromagnetics, the transducers have impulse responses that are not related through the time-derivative operator as in the case of antennas. Hence, we conclude that what happened in acoustics and was interpreted (or misinterpreted) as a back-propagation mechanism in Fink's work [9-11] cannot be easily extended to the vector problem of electromagnetic fields. Actually, the conversion of the frequency-domain antenna-impedance approach, shown in [12], to the time domain is not trivial in any sense. A good example is what we get in Equation (16). Here, we again stress that time-reversal procedures should be considered as signal-processing algorithms that have some useful capabilities in some situations, exactly as Bogert theoretically and practically presented in 1957 in [1]. A question now arises, what are the real useful capabilities of time-reversal algorithms? What are those observations that are seen by the researchers in this field? Namely, what are the spatial and

temporal focusing capabilities of time reversal? The rest of this paper answers those questions through practical examples.

4. Practical Examples

In this section, we carry out two types of experiments. First, we perform an experiment on a wireless system involving two antennas in an indoor environment. The impulse response of the wireless system is measured using simple equipment, as will be discussed. The temporal as well as the spatial focusing capabilities of time reversal are studied in detail. Second, we perform an experiment on a speech-processing system where we try to solve the problem of speech de-reverberation using a single input. In this experiment, the true capabilities of time-reversal procedures are exposed.

4.1 Experiment 1: Tx-Rx Wireless System

In this experiment, we attempted to measure the time-domain impulse response of a wireless system. The wireless system was considered as a two-port network, with port 1 as the terminals of the transmitting antenna and port 2 as the terminals of the receiving antenna. Assume in an indoor environment (a laboratory room) we have two antennas. One is to be used as a transmitter and the other as a receiver. We now want to test the time-reversal procedure by sending a pulse from the transmitting antenna, receive it at the receiver, and see how a time-reversal procedure can be used to overcome the impairments that will happen to the pulse in the indoor environment.

In practice, one of the main difficulties to extend time reversal from ultrasound directly to electromagnetics lies in the much higher sampling frequencies that are needed to digitize microwave signals. One way to overcome this limitation is to work only with monochromatic signals and to do phase conjugation. This solution was specifically used in [12] and [14]. The mentioned methodology to overcome the difficulty to digitize high-frequency signals is based on dropping the time dependence and using harmonic signals that can be processed in the frequency domain. The question is, what is the time-reversed version of a cosine wave? Dropping the time variable to eliminate the need of high-speed analog-to-digital converters makes time-reversal techniques lose their significance. In order to overcome this limitation and at the same time measure and sense the signals in the time domain, a simple workaround is presented in this paper. The measurements in this experiment were done in the frequency domain using a vector network analyzer that is commonly found in most radio-frequency research labs. The frequency-domain measurements were numerically transformed to the time domain.

4.1.1 Equipment

- A two-port vector network analyzer (VNA): an Agilent N5230-A PNA-L Network Analyzer was used, with its automatic calibration kit.

- Two antennas: different sets of antennas were used, including microstrip patches, helical antennas, Yagi antennas, and bi-blade antennas [57].
- A set of coaxial cables and SMA connectors.
- A general-purpose computer.

Figures 8 and 9 show the equipment used in this experiment, as well as the layout of the room in which the wireless channels were established.

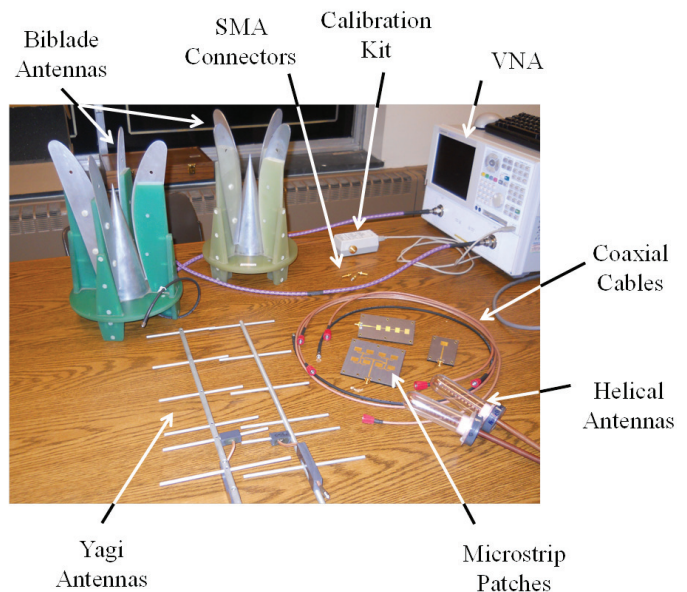


Figure 8. The equipment used in Experiment 1.

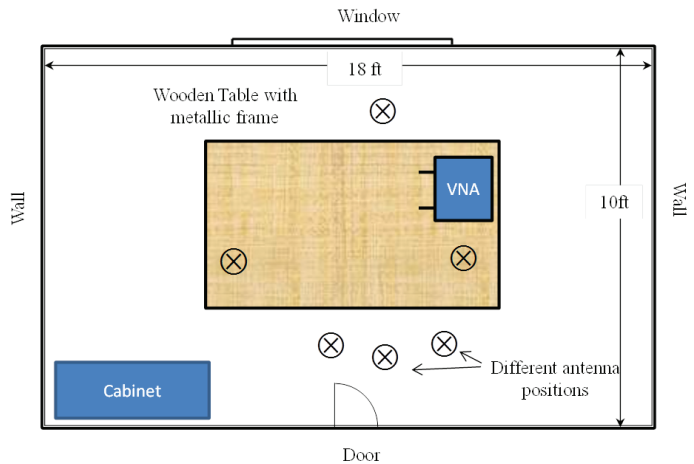


Figure 9. The layout of Experiment 1.

4.1.2 Procedure

1. The vector network analyzer was calibrated. The settings of the frequency sweep were adjusted to be from 800 MHz to 12 GHz with a step of 14 MHz (i.e., 801 points were used).
2. After the vector network analyzer was calibrated, the two ports of the vector network analyzer were connected through a female-female SMA connector.
3. The measurements of the four complex entries of the 2×2 S matrix were saved (the file could be saved as an `s2p` file).
4. Steps 2 and 3 were repeated for different sets of cables:
 - a. Long connector: a male-male transition was used as an extension to the connector of Step 2.
 - b. A 3.66 ft flexible coaxial cable.
 - c. Three rigid coaxial cables with lengths of 2.62 ft, 3.66 ft, and 6.62 ft.
5. The cables were replaced with the wireless channel by connecting port 1 to the transmitting antenna and port 2 to the receiving antenna.
6. Steps 2 and 3 were repeated for the available sets of antennas.
7. One of the antennas was moved to different locations as indicated in Figure 9, and the response at each location was measured.

4.1.3 Observations

The complex vector-network-analyzer data represent a very rich data set that can be used intelligently to get the time-domain impulse response between the two ports of the vector network analyzer. Despite the relatively large bandwidth required, the availability of such equipment nowadays makes it practical to use the methodology presented here, at least for experimental purposes. A simple inverse Fourier transform can be applied to the complex S_{21} value. Before the inverse Fourier transform is applied, the measurement errors are reduced and the causality of the physical impulse responses is enforced using a simple approach. This approach depends on relating the real and imaginary parts of the measured frequency-domain data through the Hilbert transform [55]. Applying the mentioned approach, a causal impulse response of each channel is calculated as follows:

$$h_{mn}(t) = F^{-1}\{S_{mn}\}, \quad m=1,2, \quad n=1,2, \quad (22)$$

where $F^{-1}\{\bullet\}$ is defined as

$$\begin{aligned} F^{-1}\{S_{mn}\} &= \mathfrak{F}^{-1}\{\Re(S_{mn})\} + \mathfrak{F}^{-1}\{-j\mathcal{H}[\Re(S_{mn})]\} \\ j &= \sqrt{-1}, \end{aligned} \quad (23)$$

where $\Re\{\bullet\}$ denotes the real part, $\mathfrak{F}^{-1}\{\bullet\}$ denotes the inverse Fourier Transform, and $\mathcal{H}[\bullet]$ denotes the Hilbert transform. In all measurements, the complex values of S_{21} and S_{12} are identical. This proves that all of the established channels are reciprocal. This observation is expected from Equations (19) and (20), and is very similar to what was given in [54]. It was clarified in the previous section that this happens only because of the generality of Equation (16), which relates the receiving and transmitting patterns of any kind of antenna. However, this observation does not contradict the argument that a single-antenna system is non-reciprocal: it actually enforces the necessity of studying time reversal in electromagnetics on a terminal-to-terminal basis only, and not as a backward propagation of fields.

The dc component in all of the calculated impulse responses was zero, since the bandwidth of the data set covered a limited band, from 800 MHz to 12 GHz. This band was chosen since it covered most of the personal wireless communication systems, as well as the UWB standard of the FCC. The measurement results of the female-female SMA connection are shown in Figure 10. In Figure 10a, the magnitude of the four entries of the 2×2 S matrix are shown with a dB scale, while in Figure 10b, S_{21} is specifically shown in magnitude and phase. The impulse response in this case was almost a pure impulse, but with no dc component, as expected. The signal shown in Figure 10c could be considered to be the exciting impulse in the wireless channels of the following steps. Note that the impulse response was perfectly causal, although it was calculated from band-limited frequency-domain data. This causality results from enforcing that imaginary part of the measured data be equal to the Hilbert transform of the real part. The impulse responses calculated for the setups where ports 1 and 2 of the vector network analyzer were connected directly through a cable or a connector were almost identical in shape. The different delays and amplitude changes, shown in Figure 10d, represented the different lengths and different losses of the cables and connectors. For example, the speed of wave propagation inside the rigid coaxial cable could be calculated from the different curves of Figure 10d. The three different lengths of the same type of cable gave the same speed, approximately 0.689 ft/ns.

The measurement results for the wireless channels are shown in Figures 11-14. Those four figures are organized in the same way. Parts a of these figures show the measured results on

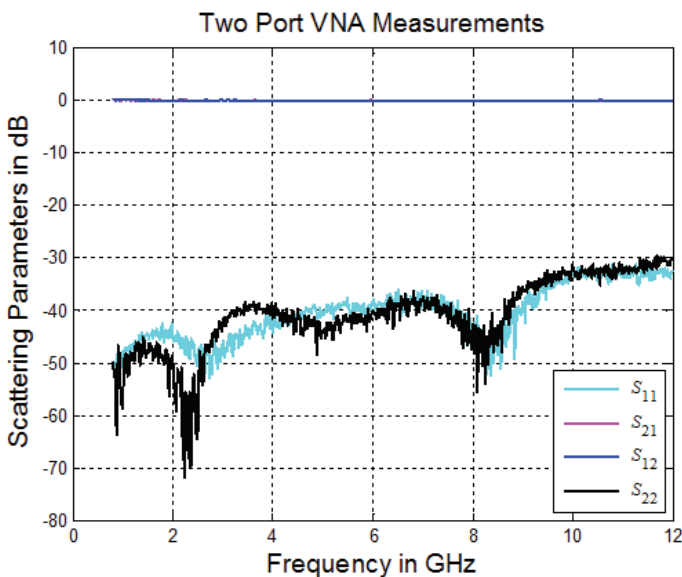


Figure 10a. The direct connection of the two ports: frequency-domain measurements with the vector network analyzer.

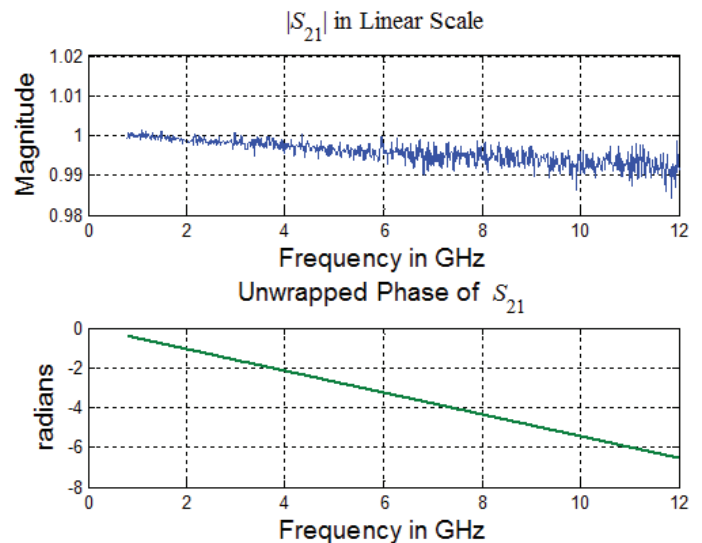


Figure 10b. The direct connection of the two ports: the S_{21} magnitude and phase on a linear scale.

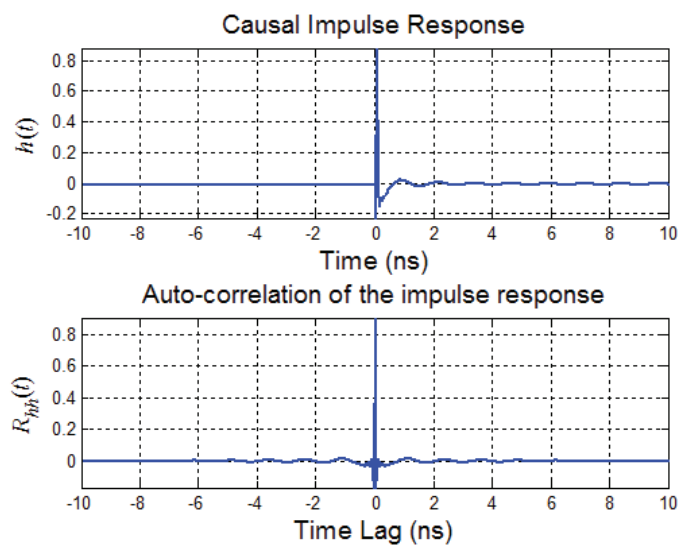


Figure 10c. The direct connection of the two ports: the time-domain response and its autocorrelation function, representing the time-reversal output.

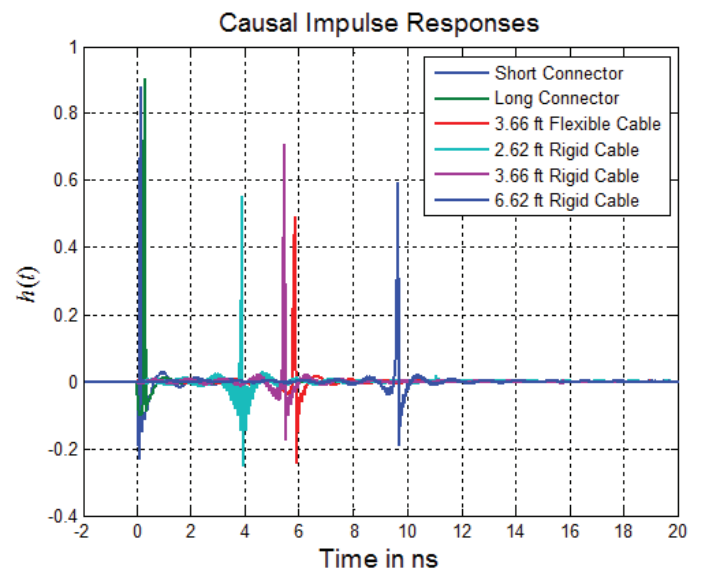


Figure 10d. The direct connection of the two ports: the time-domain responses of different cables and connectors.

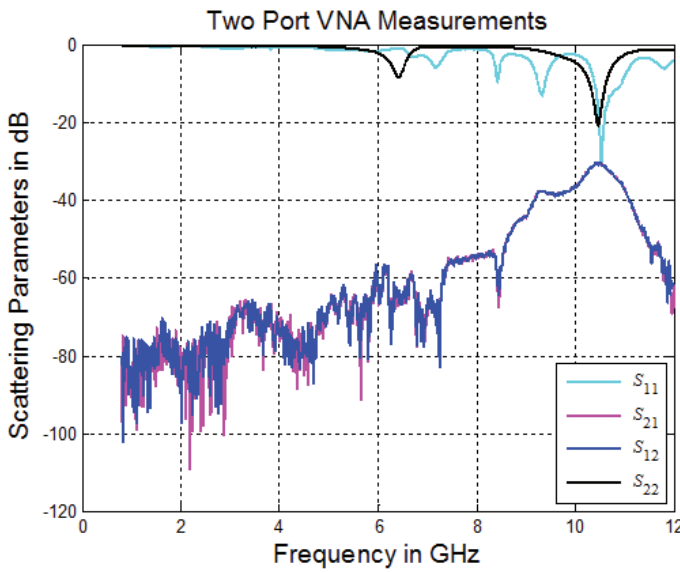


Figure 11a. The wireless connection of the two ports using microstrip patch antennas: frequency-domain measurements with the vector network analyzer.

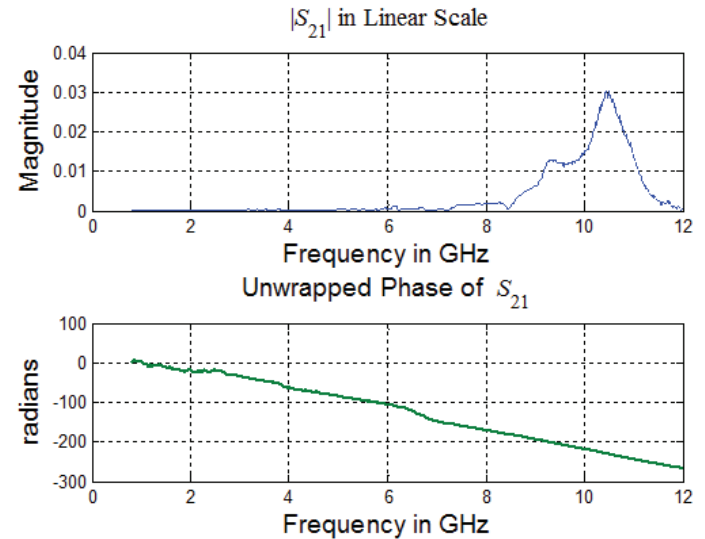


Figure 11b. The wireless connection of the two ports using microstrip patch antennas: the S_{21} magnitude and phase on a linear scale.

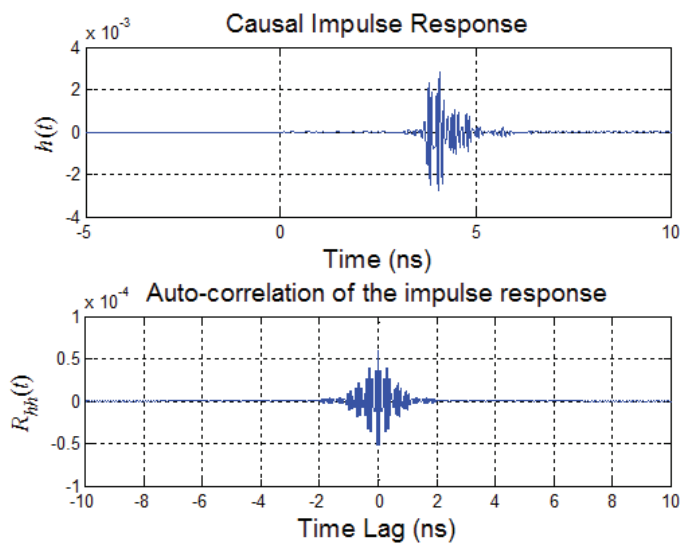


Figure 11c. The wireless connection of the two ports using microstrip patch antennas: the time-domain response and its autocorrelation function, representing the time-reversal output.

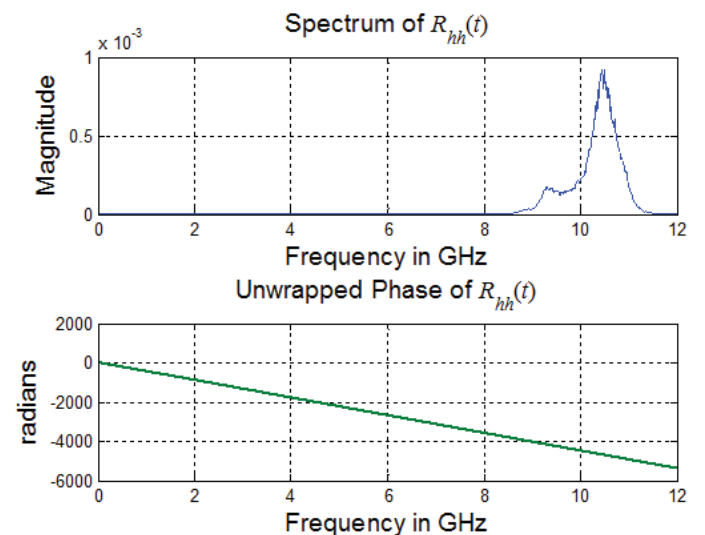


Figure 11d. The wireless connection of the two ports using microstrip patch antennas: the Fourier transform of the time-reversal output, which represents the square of the magnitude S_{21} , but with linear phase.

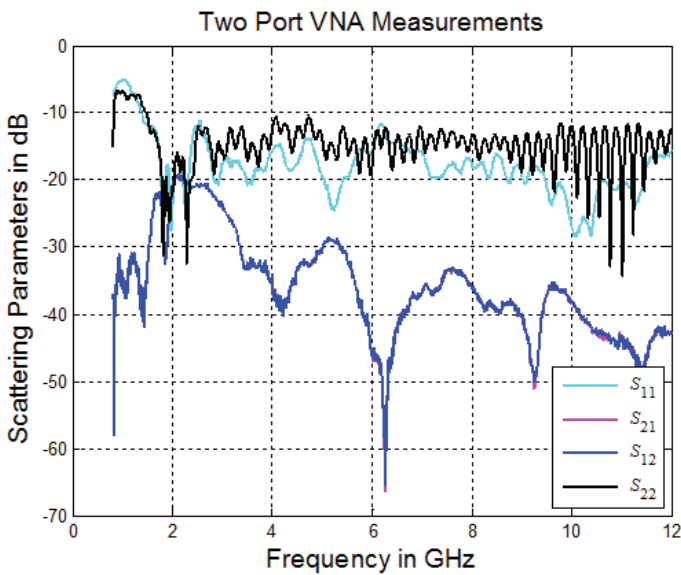


Figure 12a. The wireless connection of the two ports using the bi-blade antennas: the frequency-domain measurements with the vector network analyzer.

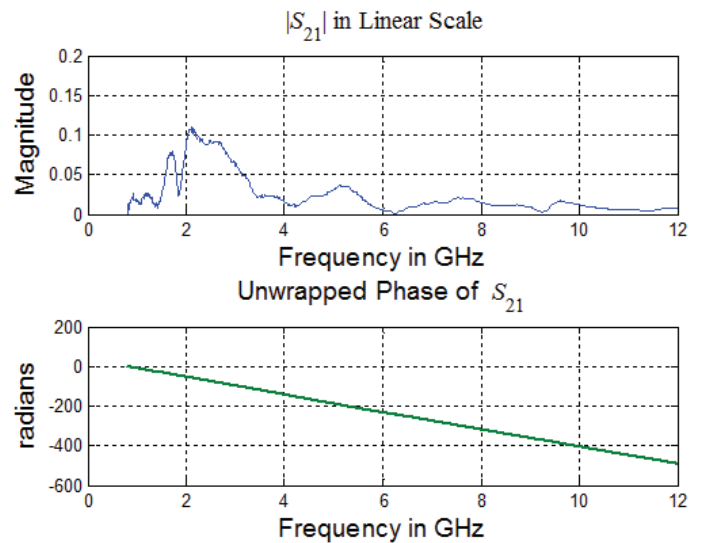


Figure 12b. The wireless connection of the two ports using the bi-blade antennas: the S_{21} magnitude and phase on a linear scale.

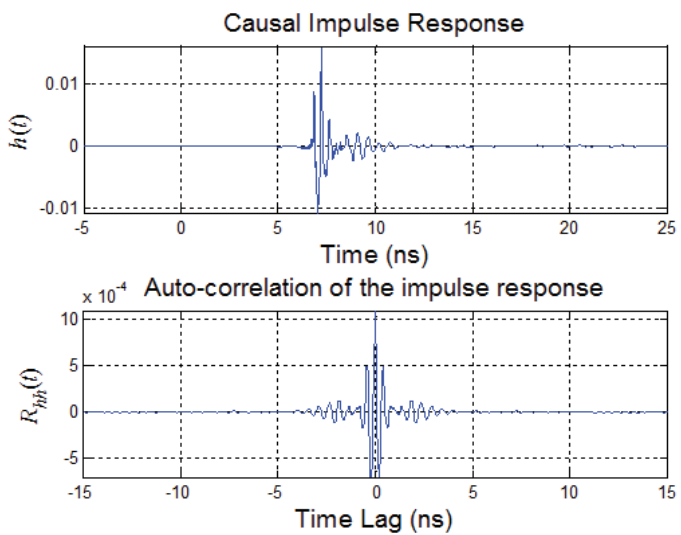


Figure 12c. The wireless connection of the two ports using the bi-blade antennas: the time-domain response and its autocorrelation function, representing the time-reversal output.

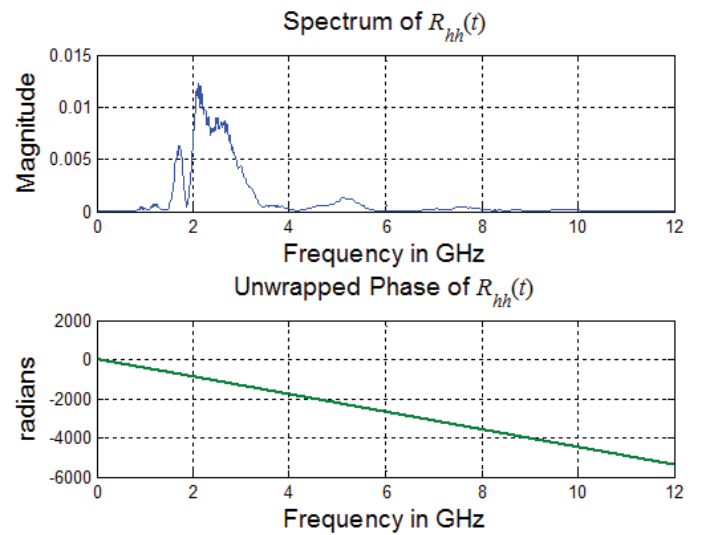


Figure 12d. The wireless connection of the two ports using the bi-blade antennas: the Fourier transform of the time-reversal output, which represents the square of the magnitude S_{21} , but with linear phase.

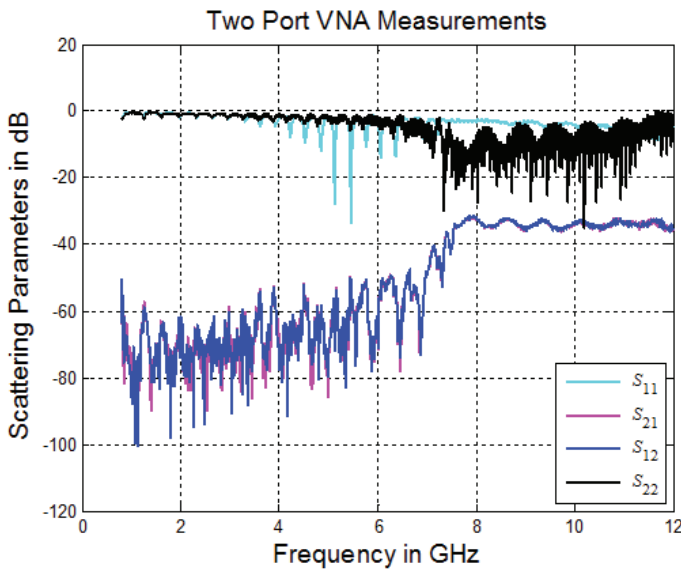


Figure 13a. The wireless connection of the two ports using the helical antennas: the frequency-domain measurements with the vector network analyzer.

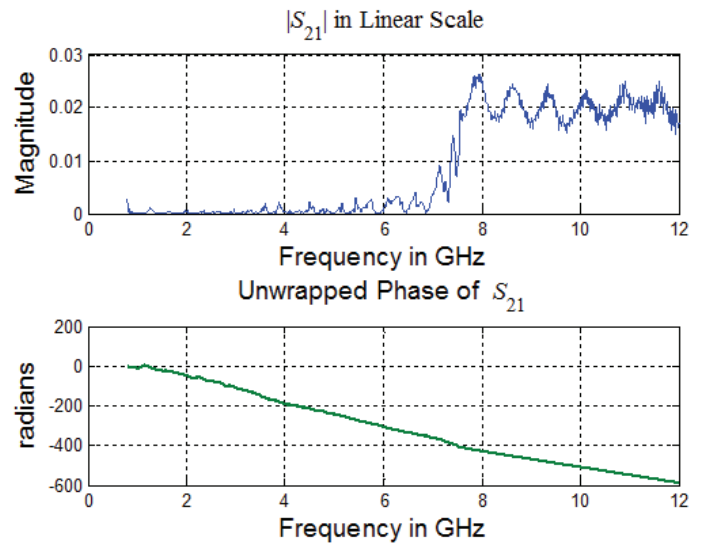


Figure 13b. The wireless connection of the two ports using the helical antennas: the S_{21} magnitude and phase on a linear scale.

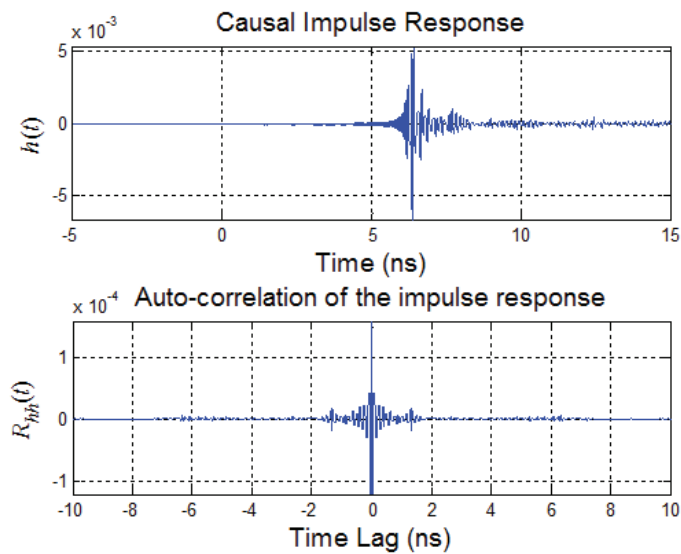


Figure 13c. The wireless connection of the two ports using the helical antennas: the time-domain response and its autocorrelation function, representing the time-reversal output.

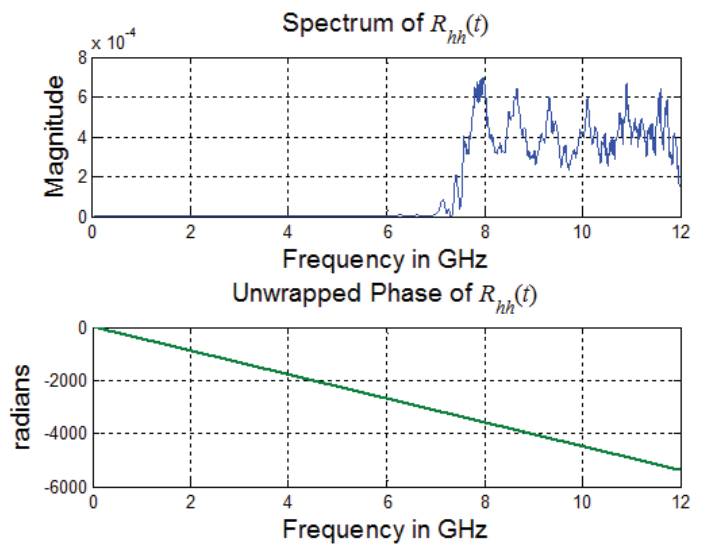


Figure 13d. The wireless connection of the two ports using the helical antennas: the Fourier transform of the time-reversal output, which represents the square of the magnitude S_{21} , but with linear phase.

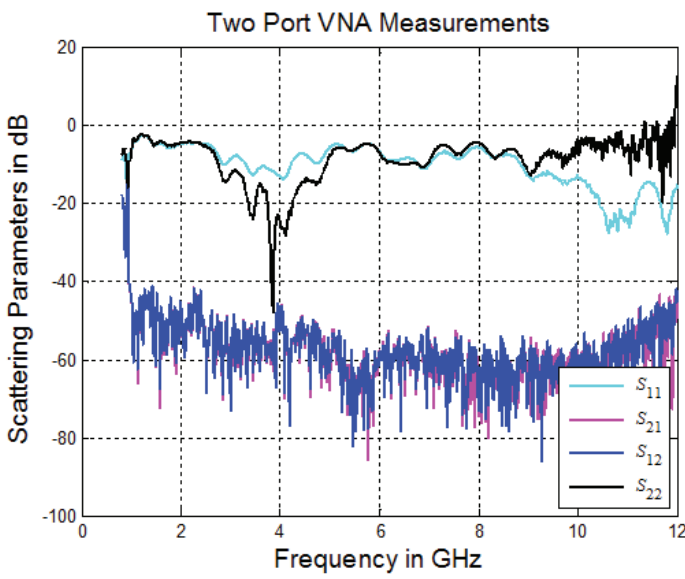


Figure 14a. The wireless connection of the two ports using the Yagi antennas: the frequency-domain measurements with the vector network analyzer.

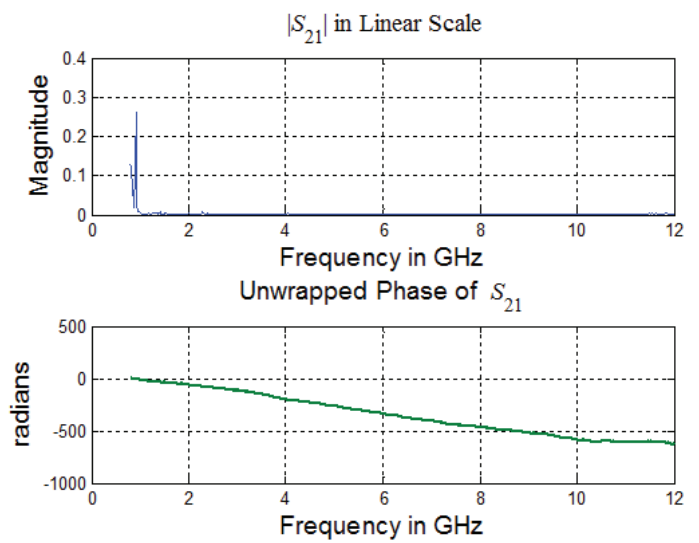


Figure 14b. The wireless connection of the two ports using the Yagi antennas: the S_{21} magnitude and phase on a linear scale.

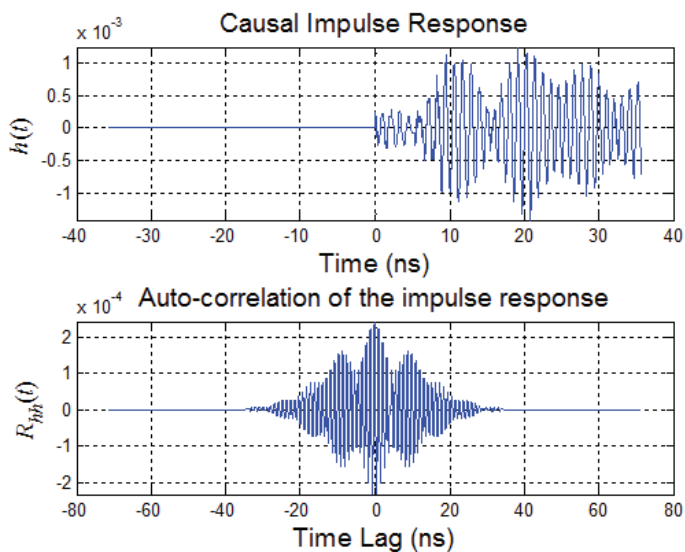


Figure 14c. The wireless connection of the two ports using the Yagi antennas: the time-domain response and its auto-correlation function, representing the time-reversal output.

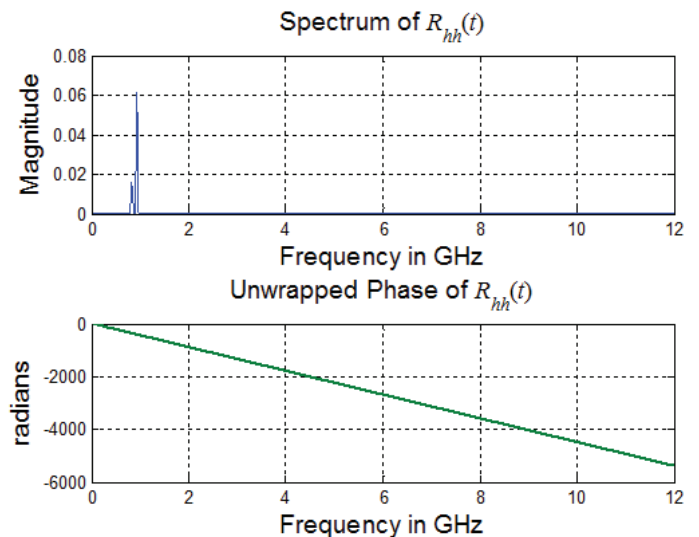


Figure 14d. The wireless connection of the two ports using the Yagi antennas: the Fourier transform of the time-reversal output, which represents the square of the magnitude S_{21} , but with linear phase.

the vector network analyzer with a dB scale. In parts c of these figures, the causal time-domain impulse response, $h(t)$, which was calculated using Equation (22), is shown in the upper part, whereas the autocorrelation function, $R_{hh}(t)$, is shown in the lower part. The magnitude and phase of the measured S_{21} values are shown in parts b for comparison with the Fourier transform of $R_{hh}(t)$, which is shown in parts d.

It was clear that the S_{21} (and S_{12}) values shown in Figures 11a, 12a, 13a, and 14a represented the multiplication of the antenna's frequency response by the environment's frequency response. For example, Figure 11a shows the results of the wireless channel using the patch antennas. It was clear from the S_{11} value that the patches were not radiating in the whole band from 800 MHz to 12 GHz. The low value of S_{21} at low frequencies was thus definitely due to the antenna and not the environment. The same thing applied for the case of the helical antennas shown in Figure 13, and the Yagi antenna shown in Figure 14. In the case of the bi-blade antennas shown in Figure 12, the S_{11} and S_{22} values of the antennas showed a very good antenna response in the entire frequency band. Actually, the bi-blades are one of the few antenna types that can be really considered as truly ultra-wideband antennas [57]. This means that the minima of S_{21} and S_{12} in Figure 12a are due to the room's response and not the antenna's response. After applying the time-domain transformation, the impulse responses of each channel were calculated, and the results of a time-reversal procedure could be tested, as follows:

$$\begin{aligned} R_{hh}(t) &= h_{left-right}(t) \otimes h_{right-left}(t) \\ &= h_{21}(-t) \otimes h_{12}(t) \\ &= F^{-1}\{S_{21}^*\} \otimes F^{-1}\{S_{12}\}. \end{aligned} \quad (24)$$

A simple comparison could be made between the time-reversal output, $R_{hh}(t)$, and the exciting impulse shown in the upper part of Figure 10c. Furthermore, a comparison between the exciting impulses and the time-reversal outputs could be made in the frequency domain with the aid of parts b and d of Figures 11-14. It was easy to use the available data to find the cross-correlation properties of the time-domain impulse responses of different channels. For example, one of the bi-blade antennas was moved in the room to record different impulse responses at different locations. The cross-correlation properties of the different impulse responses were calculated, as shown in Figures 15 and 16, and discussed in the conclusion, below.

4.1.4 Conclusions of Experiment 1

The temporal and spatial focusing capabilities, if any, of the time-reversal procedure in wireless channels are now exposed.

4.1.4.1 Temporal Focusing

Recalling Figure 2, we see that the autocorrelation of different impulse responses vary in width according to the original function itself. The narrowest is the one shown in Figure 2g, which is the autocorrelation of random Gaussian noise. Following the time-reversal standards defined in the references mentioned in this paper, the temporal focusing of time reversal in a certain channel will be measured by how narrow in time the autocorrelation function is compared to the impulse response. Parts c of Figures 11-14 show the autocorrelation properties of the calculated impulse responses. Both the impulse response and its autocorrelation function were spread over a period of 5 ns each, i.e., there was not any time compression achieved using time reversal, exactly as in Figures 2b, 2c, 2d, and 2e. Sometimes, it is claimed that the function $R_{hh}(t)$ is approximately equal to the exciting impulse when it is narrower than $h(t)$, such as what is shown in Figure 13c, which represents the time-reversed output for the case of helical antennas. This may perhaps mislead to thoughts that the propagation has been reversed in the channel. This is totally untrue, because in the frequency domain, as shown in Figure 13d, the function is exactly equal to the square of the magnitude response of the channel. It is not related in any sense to the exciting impulse. The case for the Yagi antennas, shown in Figure 14, resembled what is shown in Figure 2b, since the S_{21} of the channel with Yagi antennas had a sharp peak at 800 MHz. This made the impulse response look like a sinusoid, and the autocorrelation function in this case was totally unrelated to the exciting impulse, neither in frequency nor in time.

4.1.4.2 Spatial Focusing

The spatial-focusing capability, claimed in most of the mentioned references, can be easily examined using the cross-correlation properties of different impulse responses that were measured at different randomly selected positions, as shown in Figure 9. In the case of Figure 15a, the two impulse responses that were measured using the bi-blade antennas at different locations are shown. The autocorrelation for each of them and their cross correlation are plotted in Figure 15b. For the case of Figure 16a, the two impulse responses were for the two different channels of the patches and the bi-blades at different locations. The impulse responses in this case had a significant difference in amplitude. The responses in Figure 16a were therefore normalized before calculating the correlation functions to fairly judge the correlation properties. Even in this case, the time-domain impulse responses were still correlated, which told us that there was no spatial focusing achieved. In other words, the impulse responses from a fixed location to different locations in the room were not fully independent. We thus concluded that most of the results reported in the literature depended mainly on the media in which the results were achieved (such as the reverberant chamber shown in Figure 4), and not on the time-reversal procedure, itself.

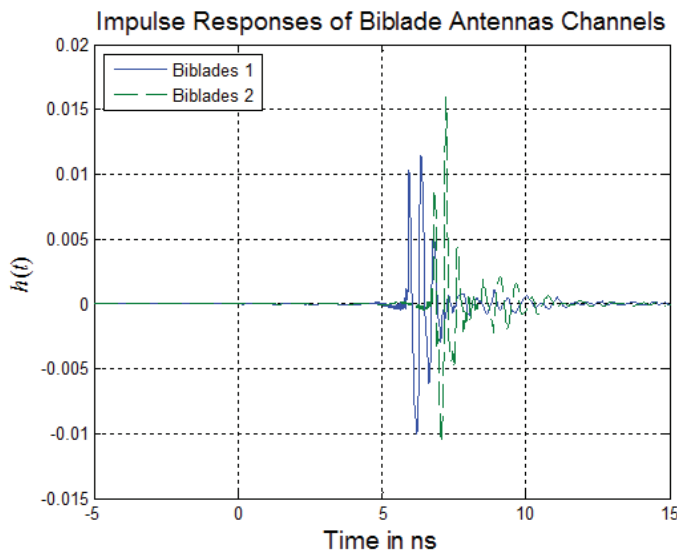


Figure 15a. The impulse responses of the bi-blade antenna channels at different locations.

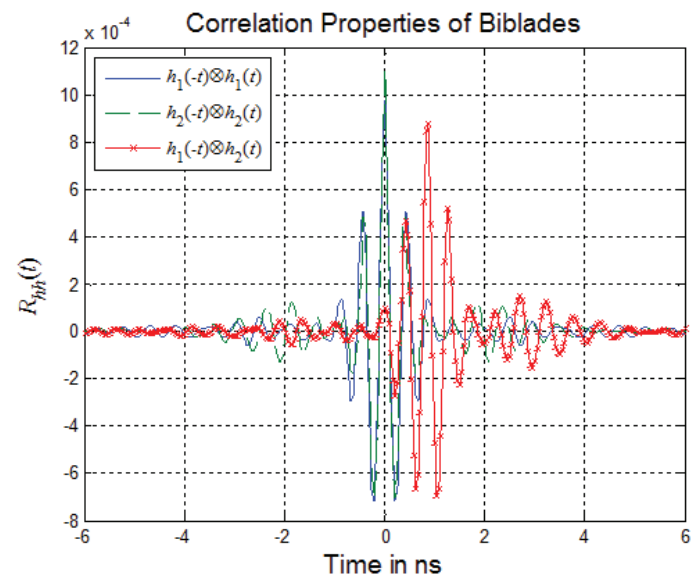


Figure 15b. The autocorrelation and cross-correlation properties of the impulse responses in Figure 15a.

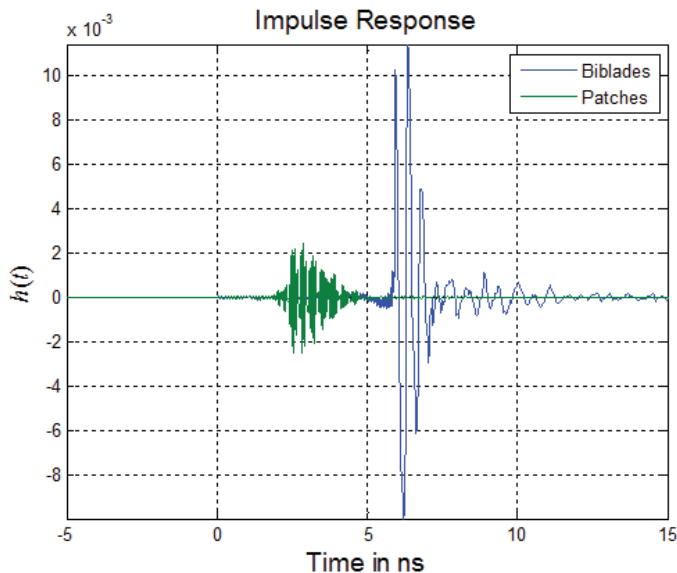


Figure 16a. The measured impulse responses of different channels, namely, the bi-blade and microstrip patch antenna channels.

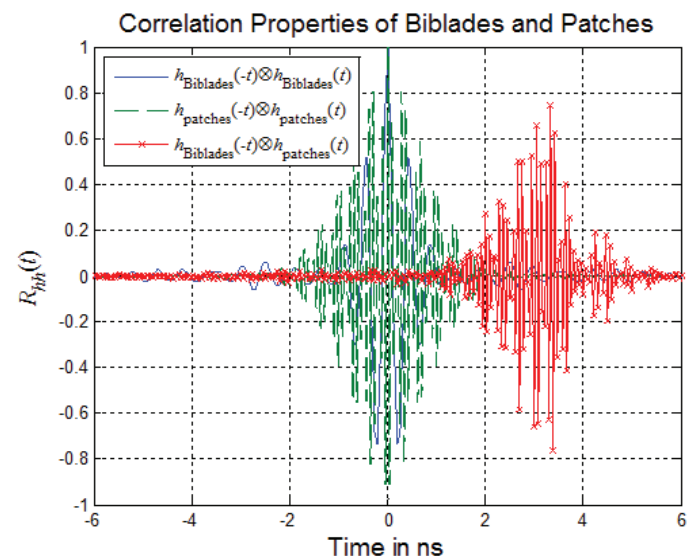


Figure 16b. The autocorrelation and cross-correlation properties of the impulse responses in Figure 16a.

Any new wireless technology to be built on time-reversal concepts, such as the time-reversal-division multiplexing proposed in [28], therefore needs a detailed study of the correlation properties of the channel impulse responses in the deployed environment. It is proposed in this paper that those correlation properties can be tested using the procedure shown in this experiment. The correlation properties should be tested only on a terminal-to-terminal basis. The concept of reversing the propagation mechanism is of no use for testing these new technologies, and it actually confuses one, rather than making the ideas of what actually is going on clearer.

4.2 Experiment 2: Speech De-Reverberation Using a Single Microphone

In this experiment, we tested the capabilities of time reversal to combat the problems of multipath propagation. The experiment was performed in a speech-processing context to facilitate the testing of the effect of time reversal on the whole system, with both subjective and objective measures.

Reverberation is the process of multipath propagation of an acoustic signal from its source to a distant microphone. The received signal generally consists of a direct sound, reflections that arrive shortly after the direct sound, and reflections that arrive after the early reverberation (commonly called late reverberation). The room effect can thus be modeled as a linear system with transfer function $h(t)$, as shown in Figure 2f. Any sound signal propagating from a source to a microphone in the environment will be convolved with that impulse response to give the received (recorded) signal at the receiver (microphone). The environmental (room) impulse response (RIR) depends on the source and receiver locations, as well as being determined by the physical structure of the room (environment). If this transfer function is exactly known, an inverse transfer function can thus be constructed to de-convolve the environmental impulse response, or in other words, to de-reverberate the sound signal. The de-reverberation problem can be viewed as the inverse filtering of the environmental impulse response. In the usual formulation of the de-convolution problem, it is assumed that the system input and system output are both known. In the case of de-reverberation, and in many other physical cases, the system input is unknown. In such cases, the problem is called blind deconvolution.

Assume a linear time-invariant system with an impulse response $h(t)$, as shown in Figure 3. In the frequency domain, an input message is modified by the complex function $H(\omega)$. To design an inverse filter that compensates for the magnitude and phase distortions caused by $H(\omega)$, one can simply design a filter with a frequency response given by

$$\begin{aligned}
H^{-1}(\omega) &= \frac{1}{\mathfrak{F}\{h(t)\}} \\
&= \frac{1}{H(\omega)} \\
&= \frac{1}{R(\omega) + jX(\omega)} \\
&= \frac{1}{R^2(\omega) + X^2(\omega)} [R(\omega) - jX(\omega)] \\
&= \frac{H^*(\omega)}{R^2(\omega) + X^2(\omega)}, \tag{25}
\end{aligned}$$

where $R(\omega)$ and $X(\omega)$ are the real and imaginary parts of $H(\omega)$, respectively. In the time domain, the inverse filter response is given by

$$h^{inv}(t) = \mathfrak{F}^{-1}\{H^{-1}(\omega)\} = h(-t) \otimes \mathfrak{F}^{-1}\left\{\frac{1}{|H(\omega)|^2}\right\}, \tag{26}$$

where $|H(\omega)| \neq 0 \forall \omega$. Practically, $h(t)$ is causal, and this directly implies that $h(-t)$ is non-causal. Therefore, a delay is usually added to $h(-t)$, as shown in Figure 3, so it becomes $h(T-t)$. If this delay is acceptable in the real-time operation of the system, there will be no problem inverting any function, even if it is a non-minimum-phase function [56]. For a signal $x(t)$ input to the original filter $h(t)$, the output of the inverse filter is therefore given by

$$\hat{x}(t) = x(t) \otimes h(t) \otimes h(T-t) \otimes \mathfrak{F}^{-1}\left\{\frac{1}{|H(\omega)|^2}\right\}, \tag{27}$$

whereas the output of the time-reversal system is given by

$$\hat{x}_{TR}(t) = x(t) \otimes h(t) \otimes h(T-t). \tag{28}$$

Comparing Equations (27) and (28) proves the fact that time reversal is an inverse filter that compensates only for the phase distortions, exactly as stated in the literature more than 50 years ago. It is therefore not clear why there currently exist research efforts on time reversal in wireless communications that expect more than just phase equalization.

In this paper, we illustrate Equations (27) and (28) using a simple experiment. *Audacity* is a free software package available on the World Wide Web that can be used for audio editing and recording [58]. *Audacity* has a built-in function for reverberation (*GVerb*). The parameters of the environment, including room size, RT60 (which is the time after which all reflections fall by 60 dB below the maximum amplitude), delay time, etc., can be modified in the program. In this experiment, the reverberation function of *Audacity* was used to reverberate a clean speech segment of a female voice saying, “She has your dark suit in greasy wash water all year” [59]. The time-domain clean speech signal is shown in the upper part of Figure 19. A short-time Fourier transform (STFT) was applied to the clean speech, and this is shown in the upper-right part of Figure 19. Assume that the goal was to de-reverberate the reverberated signal. The question was how to do this, assuming that the only available signal was the reverberated speech. This reverberated speech is shown in the lower part of Figure 19, along with its short-time Fourier transform. There are two ways to do this, as shown in Figure 17.

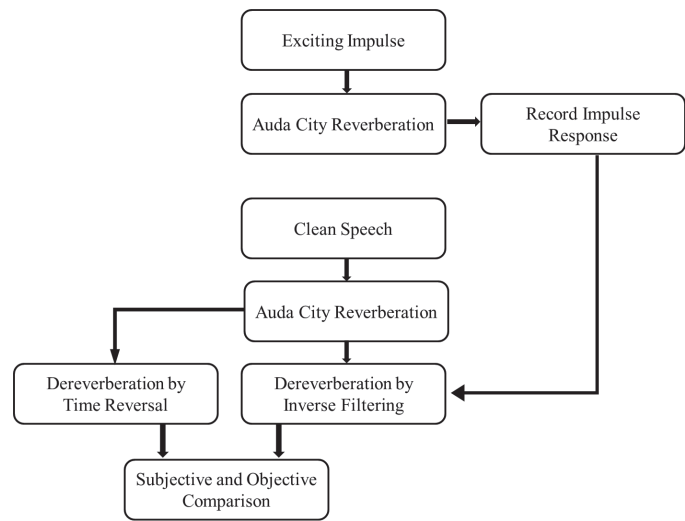


Figure 17. A flowchart of the *Audacity* software experiment.

4.2.1 De-Reverberation Using Inverse Filtering

1. Generate an impulse function using *MATLAB*. Assume that the sampling frequency is 8 kHz.
2. Apply the impulse, $\delta(t)$, to the *Audacity* program as the signal to be reverberated.
3. Record the impulse response of the reverberation function of *Audacity*, $h(t)$.
4. Apply the long clean speech signal, $x(t)$, and record its reverberated version, $x(t) \otimes h(t)$. Assume now that the clean speech is not available anymore.
5. In *MATLAB*, take the fast Fourier transform (FFT) of the impulse response and the reverberated speech.
6. Apply inverse filtering by dividing the reverberated speech by the recorded impulse response in the frequency domain according to Equation (25), to get the estimated speech, $\hat{X}(f)$.
7. Take the inverse FFT of the estimated speech to get the estimated speech in the time domain, $\hat{x}(t)$, as in Equation (27). The output of this step is shown in the upper part of Figure 20.
8. Compare the estimated speech and its short-time Fourier transform to the clean speech.

4.2.2 De-Reverberation Using Time Reversal

This procedure can be explained using the block diagram of Bogert’s experiment, shown in Figure 3. In this case, the impulse response does not need to be recorded first, because it is assumed that the transmission medium is available for the signal to pass through one more time after time reversal. This explains why Bogert concluded that time reversal is suitable only for “**bisectable** transmission circuits and networks.” In Bogert’s experiments, he did not record the transmission’s impulse response. To the contrary, he applied his time-reversed signal to the transmission medium, again. In conclusion, if the system is “bisectable,” this is equivalent to recording its impulse response.

1. Apply the clean speech signal, $x(t)$, to the reverberation function of *Audacity*, $h(t)$, and record the reverberated speech, $x(t) \otimes h(t)$.
2. Using *MATLAB* or *Audacity*, flip the reverberated speech in time.
3. Apply the flipped version of the reverberated speech, $y(t)$, to the same reverberation function again, as follows:

$$y(t) = TR\{x(t) \otimes h(t)\} = x(-t) \otimes h(-t), \quad (29)$$

$$\hat{x}_{TR}(-t) = y(t) \otimes h(t) = x(-t) \otimes h(-t) \otimes h(t).$$

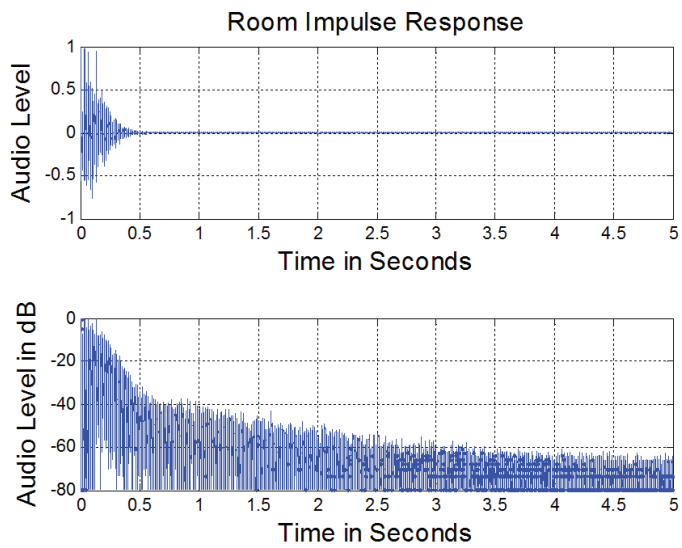


Figure 18a. The acoustic room impulse response, calculated using an impulse excitation with the *Audacity* software.

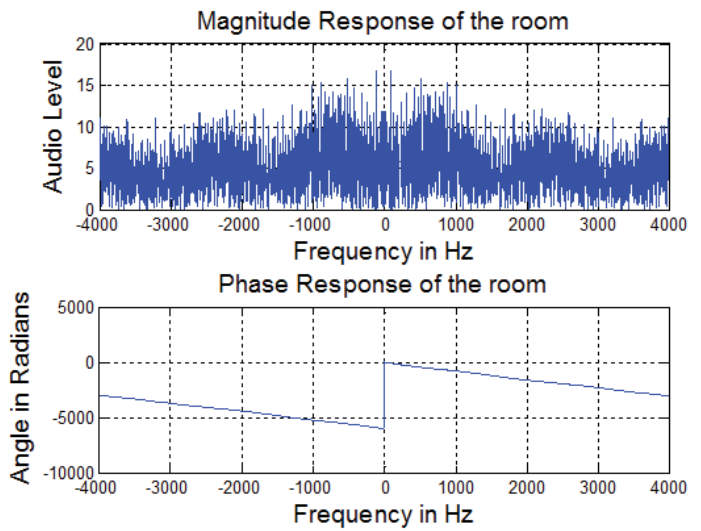


Figure 18b. The magnitude and phase responses of the room impulse response signal shown in Figure 18a.

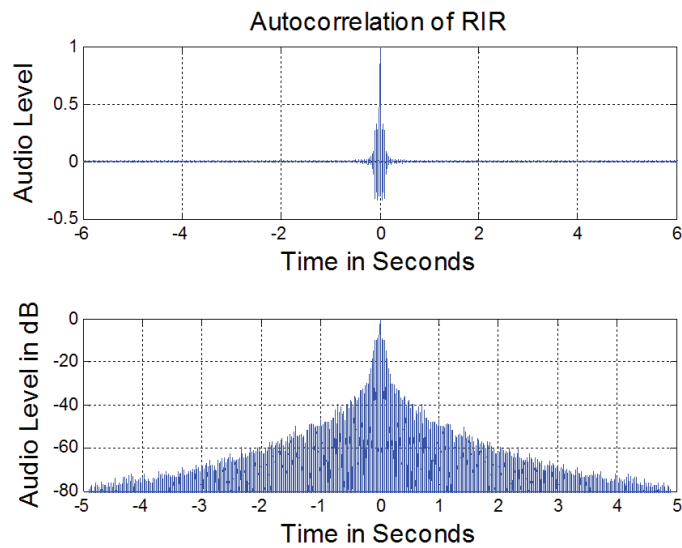


Figure 18c. the time-reversal output represented by the autocorrelation function of the room impulse response of Figure 18a.

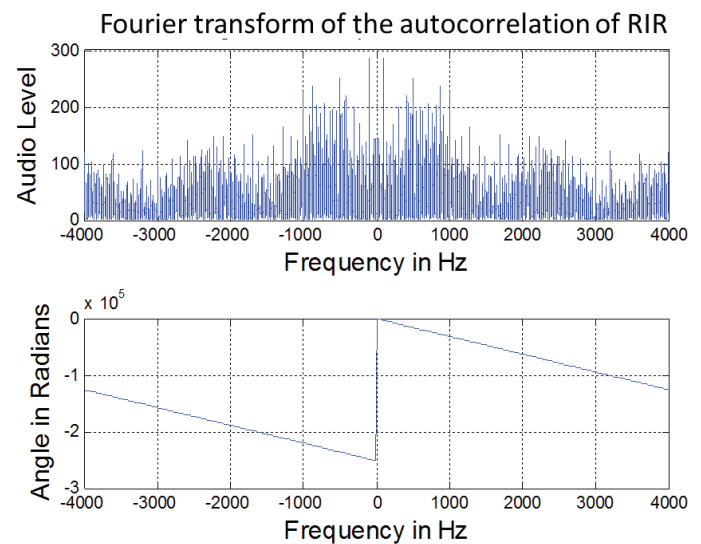


Figure 18d. The magnitude and phase responses of the autocorrelation function of Figure 18c.

4. Flip the output of step 3 in time, and record it as the time-reversal estimated speech, $\hat{x}_{TR}(t)$. This is exactly as given by Equation (28), except for the arbitrary delay, T . The output of this step is shown in the lower part of Figure 20.
5. Compare the time-reversal estimated speech and its short-time Fourier transform to the clean speech.

4.2.3 Conclusion of Experiment 2

De-reverberation using inverse filtering is very successful. This was clear from the comparison of Figures 19 and 20. It is also clear from subjective testing of the quality of the estimated speech using inverse filtering that the estimated speech is exactly similar to the original clean speech. The recorded impulse response, which is shown in Figure 18, was completely deconvolved from the reverberated speech using simple division in the frequency domain (provided that there were no zeros on the frequency axis). Note that from the phase of the Fourier transform of the environmental impulse response, shown in the upper-right part of Figure 17, we could deduce that the environmental impulse response was a non-minimum-phase function. This means that inversion of non-minimum phase functions is possible if offline processing is possible, as in this experiment.

The impulse response of reverberation environments that results from multipath propagation of waves in a non-dispersive media suffers from severe variations in the magnitude of the frequency response, whereas there are not as much variations in the phase response. This is clear not only from Figure 18, but also from the phase responses of the channels measured in Experiment 1, as shown in Figures 11-14. De-reverberation using time reversal only compensates for the nonlinearity of the phase response of the room (which is not very effective), but at the same time, it squares the effect of those rapid variations of the magnitude response. This was clear from the subjective as well as the objective comparison of the speech signal estimated using time reversal, which is shown in the lower part of Figure 20. The relative compression of the time-domain impulse response shown in the lower part of Figure 18 was not very effective in inverting the effects of the room. This is expected from the shape of the Fourier transform of the compressed version of the impulse response, as shown in the same figure. The same experiment can be repeated using a database of measured acoustic impulse responses of different environments, which is available in [60].

5. Conclusion

In this paper, time reversal in electrical engineering has been studied in detail in the light of the basic fundamentals of signals and systems and electromagnetics. The earliest application of time reversal in electrical engineering goes back to

the 1950s of the last century. From the literature review, two views of time reversal have been identified and differentiated. The definition that defines time reversal as a backward-propagation mechanism of waves was found to have some problems. The non-reciprocity of a single antenna questions the sensibility of applying such a methodology. The appropriate definition of time reversal that scientifically makes sense is found to be, “time reversal is a signal-processing algorithm that compensates for the phase distortion of transmission media of **uniform** characteristics.” This definition is exactly what was used in the period of the 1950s to the 1980s of the last century. The interesting application of time reversal in acoustics in the beginning of the 1990s of the last century depends mainly on a huge array of sensors used as the time-reversal mirror. The application of a large number of sensors is the main source of the temporal and spatial focusing that occurred in those experiments. The large numbers of sensors, along with the flipping-in-time procedure applied at each sensor, represent a wideband beamforming process. A simple real-life example was given in the introduction of this paper to explain the difference between the effect of the wideband beamforming process and the real reversal of the propagation mechanism.

The difference between the single-antenna and the two-antenna reciprocity relations was explained in detail in this paper. We showed in this paper why a two-antenna system is reciprocal, while a single-antenna system is not. The conclusion of the theoretical part of the paper was verified by performing two experiments in the laboratory. A century-bandwidth bi-blade antenna was used in the first experiment to establish a 175% bandwidth indoor wireless channel. The established channel and its measured time-domain response have exposed the real capabilities of time reversal in terms of temporal and spatial focusing. The autocorrelation and the cross-correlation of time-domain impulse responses were proven to be suitable tools for testing the spatial and temporal focusing capabilities of a technique. There are efforts to apply time reversal in wireless communications to combat multipath fading. A speech-processing experiment was carried out to illustrate the effect of the time-reversal procedures in combating sound reverberation, which is exactly similar to multipath fading in wireless channels. Time reversal showed very poor performance in enhancing the impairments resulting from the nonuniform magnitude characteristics of the transmission media.

6. Appendix

For a two-port network, the transmission matrix, or what is sometimes called the ABCD matrix, is defined by

$$\begin{bmatrix} V_1 \\ I_1 \end{bmatrix} = \begin{bmatrix} A & B \\ C & D \end{bmatrix} \begin{bmatrix} V_2 \\ I_2 \end{bmatrix}, \quad (30)$$

where V_1 , I_1 , V_2 , and I_2 are defined in Figure 21. The usefulness of the transmission matrix lies in its ability to separate the input and output voltages and currents. This is very beneficial

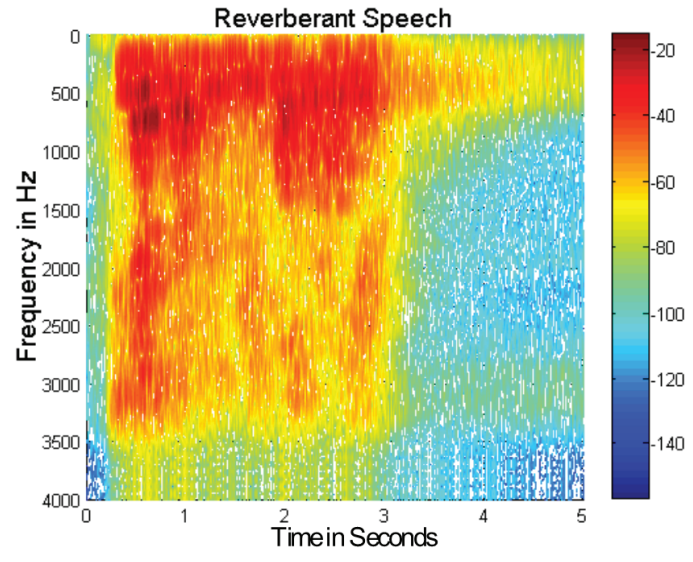
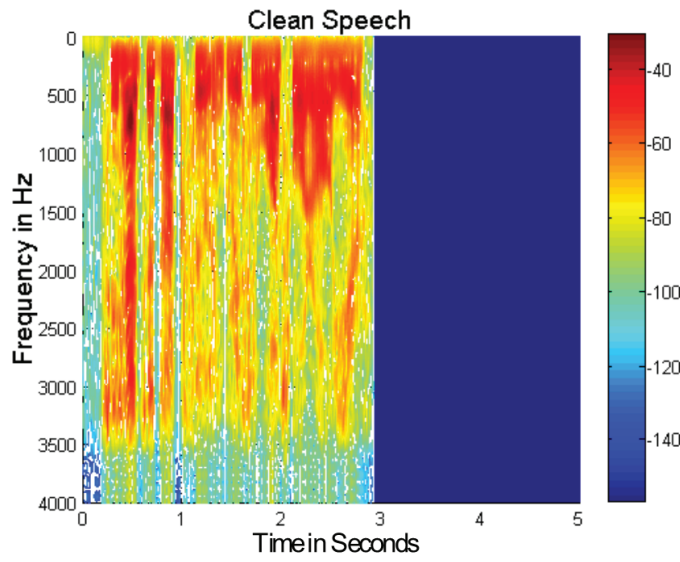
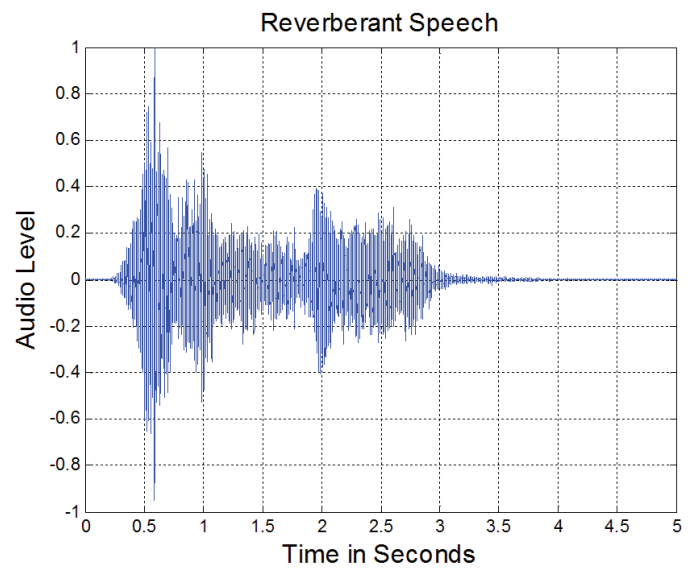
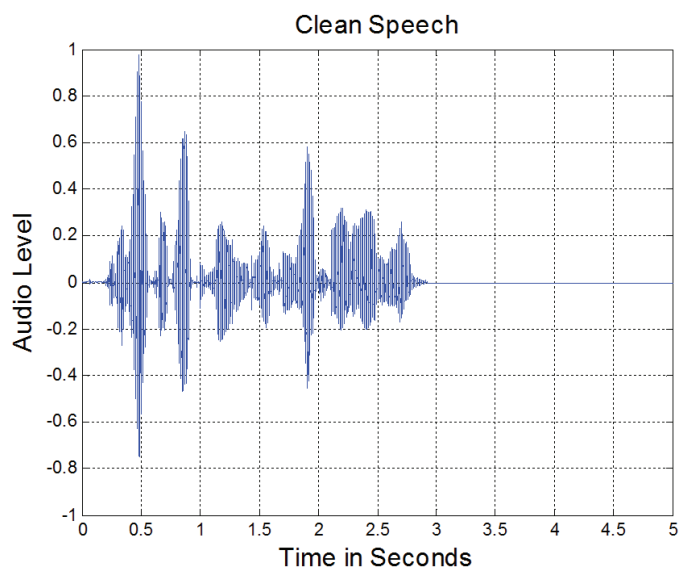


Figure 19a. The clean speech signal in the time domain and its spectrogram.

Figure 19b. The reverberant speech signal in time domain and its spectrogram.

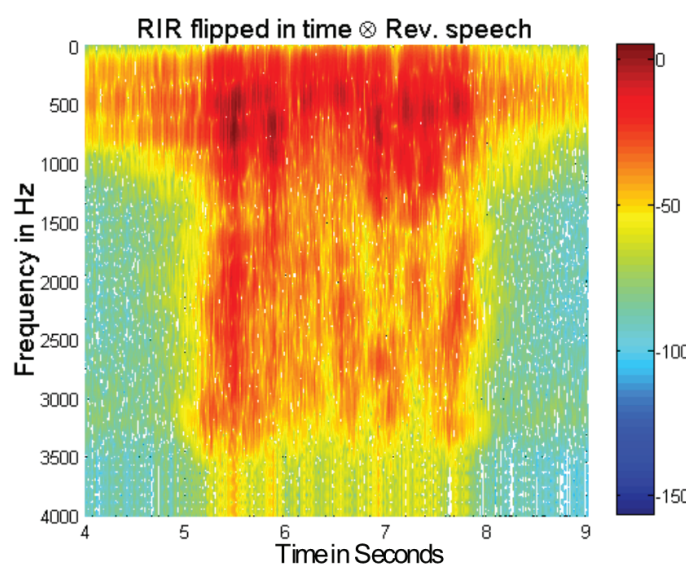
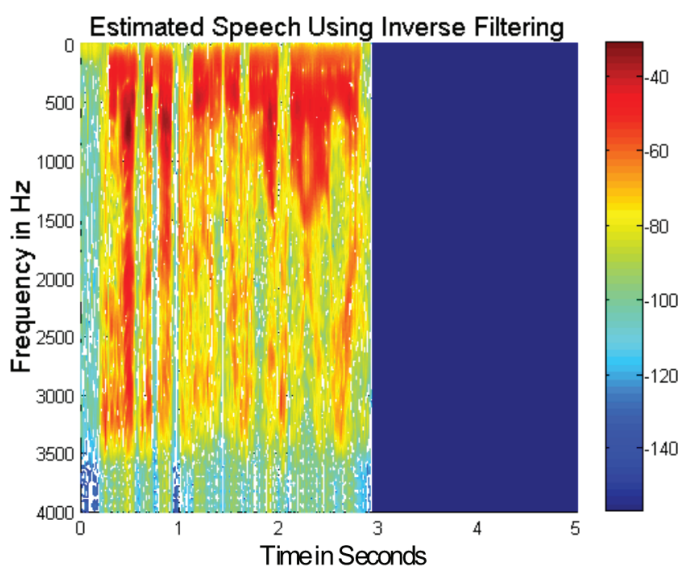
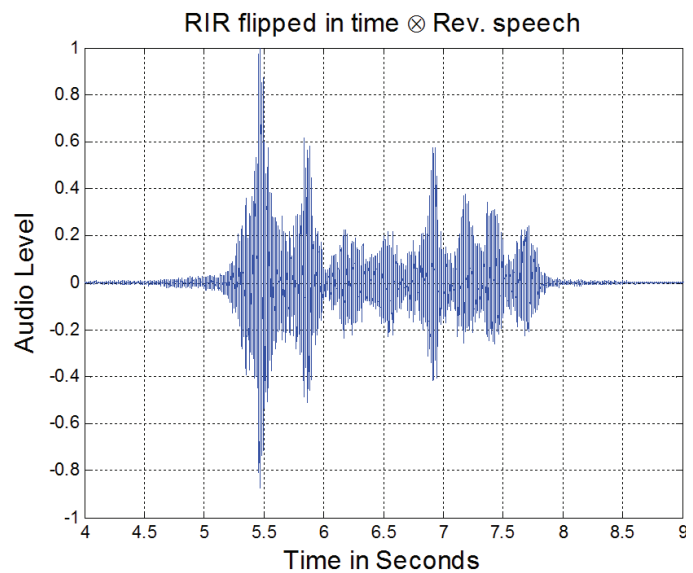
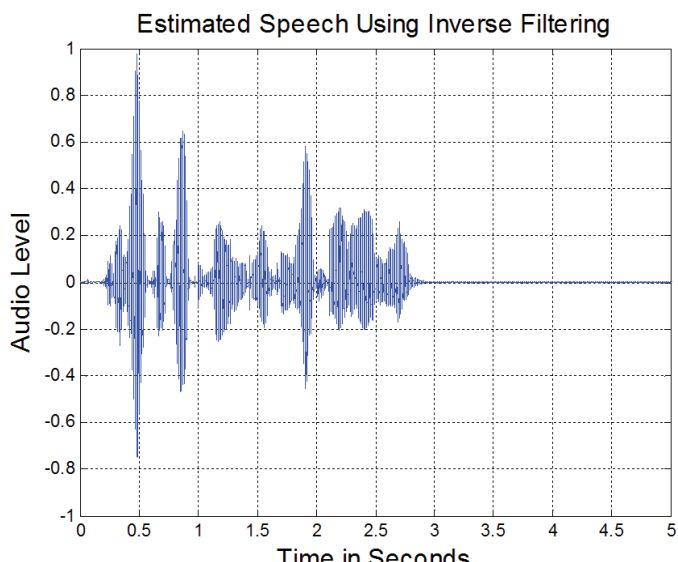


Figure 20a. The estimated speech signal using inverse filtering and its spectrogram.

Figure 20b. The estimated speech signal using time reversal and its spectrogram.

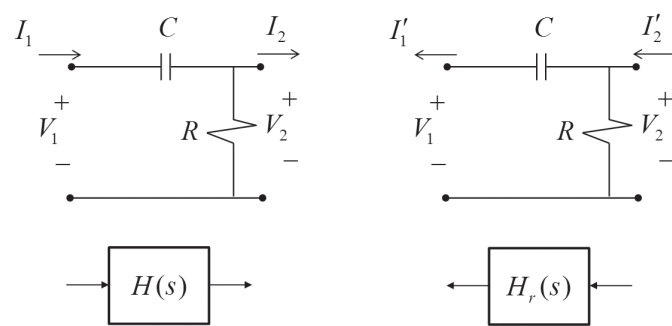


Figure 21. The relationship between the impulse response and the transmission matrix of reciprocal networks.

when successive networks are connected in cascade. For the simple RC network shown in Figure 21, the ABCD matrix is given by

$$A = \frac{V_1}{V_2} \Big|_{I_2=0} = \frac{1+RCs}{RCs}, \quad (31)$$

$$B = \frac{V_1}{I_2} \Big|_{V_2=0} = \frac{1}{Cs}, \quad (32)$$

$$C = \frac{I_1}{V_2} \Big|_{I_2=0} = \frac{1}{R}, \quad (33)$$

$$D = \frac{I_1}{I_2} \Big|_{V_2=0} = 1, \quad (34)$$

$$\therefore \begin{bmatrix} V_1 \\ I_1 \end{bmatrix} = \begin{bmatrix} 1+RCs & 1 \\ RCs & Cs \end{bmatrix} \begin{bmatrix} V_2 \\ I_2 \end{bmatrix}, \quad (35)$$

where s is the complex frequency variable. In signals and system theory, the same network of Figure 21 can be represented as a block of a linear time-invariant system with an impulse response, $h(t)$, the Laplace transform of which is $H(s)$. Note that $H(s)$ is a function, not a matrix. Equation (35) thus directly implies that the impulse response of a two-port network can be defined in four different ways. The four possible ways to define $H(s)$ are as follows:

$$H_v(s) = \frac{1}{A} = \left[\frac{V_1(s)}{V_2(s)} \Big|_{I_2=0} \right]^{-1} = \frac{RCs}{1+RCs}, \quad (36)$$

$$H_{trans-cond}(s) = \frac{1}{B} = \left[\frac{V_1(s)}{I_2(s)} \Big|_{V_2=0} \right]^{-1} = Cs, \quad (37)$$

$$H_{trans-imp}(s) = \frac{1}{C} = \left[\frac{I_1(s)}{V_2(s)} \Big|_{I_2=0} \right]^{-1} = R, \quad (38)$$

$$H_i(s) = \frac{1}{D} = \left[\frac{I_1(s)}{I_2(s)} \Big|_{V_2=0} \right]^{-1} = 1. \quad (39)$$

Suppose that the input and output ports are switched. This implies

$$\begin{bmatrix} V_2 \\ I'_2 \end{bmatrix} = \begin{bmatrix} A' & B' \\ C' & D' \end{bmatrix} \begin{bmatrix} V_1 \\ I'_1 \end{bmatrix} = \begin{bmatrix} 1 & \frac{1}{Cs} \\ \frac{1}{R} & \frac{1+RCs}{RCs} \end{bmatrix} \begin{bmatrix} V_1 \\ I'_1 \end{bmatrix}, \quad (40)$$

where the directions of I'_1 and I'_2 are the opposite of I_1 and I_2 . Note that the matrix in Equation (40) is exactly the inverse of the matrix in Equation (35), but with the opposite sign of the off-diagonal elements. This change of sign comes from the change in current directions, as illustrated in Figure 21. It is clear that $H_v(s)$ in this case is not the same as in Equation (36), unless it is defined as the current gain and not the voltage gain. The only way $H(s)$ will not be changed after switching the input and output ports is to define $H(s)$ as the relationship between the input voltage and the output current, or vice versa, as in Equations (37) and (38). In fact, this conclusion should be expected from the derivation of the reciprocity theorem given in [61]. The reciprocity of passive electric circuits is a special case of the reciprocity theorem of fields. Simplifying what is in [61] to the special case of electric circuits, we can write, for a reciprocal network,

$$\langle V_1, I_1 \rangle = \langle V_2, I_2 \rangle, \quad (41)$$

where I_1 is the short-circuit current at port 1 due to the source applied at port 2 (V_2), and I_2 is the short-circuit current at port 2 due to the voltage source applied at port 1 (V_1). Alternatively, one can define the quantities in Equation (41) as follows: V_1 is the open-circuit voltage at port 1 due to the current source applied at port 2 (I_2), and V_2 is the open-circuit voltage at port 2 due to the current source applied at port 1 (I_1). The product $\langle V_1, I_1 \rangle$ is called the reaction at port 1 due to a source at port 2. This reaction reduces to a simple multiplication in the frequency domain, while it represents a convolution in the time domain. This is obvious if one tries to prove Equation (41) through an example. Assume that a pulse, $v_1(t)$, is applied to port 1 in Figure 21. The short-circuit current, $i_2(t)$, in the other port can be calculated in the s domain as follows:

$$I_2(s) = \frac{1}{B} V_1(s) = Cs V_1(s). \quad (42)$$

If another pulse, $v_2(t)$, is applied to port 2, the reaction to this pulse at port 1 can be calculated as

$$I_1(s) = Cs V_2(s). \quad (43)$$

From Equations (42) and (43), it is clear that

$$V_1(s) I_1(s) = V_2(s) I_2(s) = Cs V_1(s) V_2(s). \quad (44)$$

From the properties of the Laplace transform, Equation (44) in the time domain is written as

$$v_1(t) \otimes i_1(t) = v_2(t) \otimes i_2(t), \quad (45)$$

$$C \frac{dv_1(t)}{dt} \otimes v_2(t) = Cv_1(t) \otimes \frac{dv_2(t)}{dt}.$$

We therefore conclude that in the time domain, the reciprocity relationship involves the convolution of the waveforms instead of direct multiplication. For a linear time-invariant system for which the impulse response is expected to not be changing with the direction of signal flow, the impulse response should be defined either in a trans-impedance or a trans-conductance form. This is because the reaction concept, on which the reciprocity theorem depends, is defined for those forms.

7. References

1. B. P. Bogert, "Demonstration of Delay Distortion Correction by Time-Reversal Techniques," *IRE Transactions on Communications Systems*, **5**, 3, December, 1957, pp. 2-7.
2. K. E. Schreiner, H. L. Funk, and E. Hopner, "Automatic Distortion Correction for Efficient Pulse Transmission," *IBM Journal*, January, 1965.
3. J. J. Kormylo and V. K. Jain, "Two-Pass Recursive Digital Filter with Zero Phase Shift," *IEEE Transactions on Acoustics, Speech, and Signal Processing*, October, 1974, pp. 384-387.
4. R. Czarnach, "Recursive Processing by Noncausal Digital Filters," *IEEE Transactions on Acoustics, Speech, and Signal Processing*, **ASSP-30**, 3, June, 1982, pp. 336-370.
5. D. Harasty and A. Oppenheim, "Television Signal Deghosting by Noncausal Recursive Filtering," International Conference on Acoustics, Speech, and Signal Processing, **3**, April, 1988, pp. 1778-1781.
6. C. Tsai and A. T. Fam, "Efficient Linear Phase Filters based on Switching and Time Reversal," IEEE International Conference on Circuits and Systems, **3**, May, 1990, pp. 2161-2164.
7. J. H. Winters, E. Ayanoglu, I. Bar-David, R. D. Gitlin, and Chili-Lin I, "Ghost Cancellation of Analog TV Signals: With Applications to IDTV, EDTV, and HDTV," *IEEE Transactions on Circuits and Systems for Video Technology*, **1**, 1, March, 1991, pp. 136-146.
8. K. S. Yeung, K. Chen, and C. M. Kwan, "Implementing Unstable Filters via Input Signal Reversal – A State Variable Perspective," *IEEE Transactions on Circuits and Systems – I: Fundamental Theory and Applications*, **45**, 1, January, 1998, pp. 101-104.
9. M. Fink, "Time Reversal of Ultrasonic Fields – Part I: Basic Principles," *IEEE Transactions on Ultrasonics, Ferroelectrics, and Frequency Control*, **39**, 5, September 1992, pp. 555-566.
10. F. Wu, J. Thomas, and M. Fink, "Time Reversal of Ultrasonic Fields – Part II: Experimental Results," *IEEE Transactions on Ultrasonics, Ferroelectrics, and Frequency Control*, **39**, 5, September, 1992, pp. 567-578.
11. D. Cassereau and M. Fink, "Time Reversal of Ultrasonic Fields – Part III: Theory of the Closed Time-Reversal Cavity," *IEEE Transactions on Ultrasonics, Ferroelectrics, and Frequency Control*, **39**, 5, September 1992, pp. 579-592.
12. J. de Rosny, G. Lerosey, and M. Fink, "Theory of Electromagnetic Time-Reversal Mirrors," *IEEE Transactions on Antennas and Propagation*, **AP-58**, 10, October 2010, pp. 3139-3149.
13. A. Cozza, and A. Abou el-Aileh, "Accurate Radiation-Pattern Measurements in a Time-Reversal Electromagnetic Chamber," *IEEE Antennas and Propagation Magazine*, **52**, 2, April 2010, pp. 186-193.
14. G. Lerosey, J. de Rosny, A. Tourin, A. Derode, G. Montaldo, and M. Fink, "Time Reversal of Electromagnetic Waves," *Physical Review Letters*, **92**, 19, May, 2004.
15. G. Lerosey, J. de Rosny, A. Tourin, A. Derode, and M. Fink, "Time Reversal of Wideband Microwaves," *Applied Physics Letters*, **88**, 15, April, 2006, p. 154101.
16. Z. Yun and M. F. Iskander, "Time Reversal with Single Antenna Systems in Indoor Multipath Environments: Spatial Focusing and Time Compression," IEEE International Symposium on Antennas and Propagation, 2006, pp. 695-698.
17. C. Oestges, A. D. Kim, G. Papanicolaou, and A. J. Paulraj, "Characterization of Space-Time Focusing in Time-Reversed Random Fields," *IEEE Transactions on Antennas and Propagation*, **AP-53**, 1, January 2005, pp. 283-293.
18. A. Derode, A. Tourin, and M. Fink, "Ultrasonic Pulse Compression with One-bit Time Reversal through Multiple Scattering," *Journal of Applied Physics*, **85**, 9, pp. 6343-6352.
19. P. Kyritsi, G. Papanicolaou, P. Eggers, and A. Oprea, "Time Reversal Techniques for Wireless Communications," IEEE 60th Vehicular Technology Conference, **1**, September, 2004, pp. 47-51.
20. P. Kyritsi, G. Papanicolaou, P. Eggers, and A. Oprea, "MISO Time Reversal and Delay-Spread Compression for FWA Channels at 5 GHz," *IEEE Antennas and Wireless Propagation Letters*, **3**, 2004, pp. 96-99.

21. H. T. Nguyen, J. B. Andersen, and G. F. Pedersen, "The Potential Use of Time Reversal Techniques in Multiple Element Antenna Systems," *IEEE Communications Letters*, **9**, 1, January, 2005, pp. 40-42.
22. P. Kyritsi, and G. Papanicolaou, "One-Bit Time Reversal for WLAN Applications," IEEE 16th International Symposium on Personal, Indoor and Mobile Radio Communications, September, 2005, pp. 532-536.
23. H. T. Nguyen, I. Z. Kovács, and P. C. F. Eggers, "A Time Reversal Transmission Approach for Multiuser UWB Communications," *IEEE Transactions on Antennas and Propagation*, **AP-54**, 11, November, 2006, pp. 3216-3224.
24. H. T. Nguyen, J. B. Andersen, G. F. Pedersen, P. Kyritsi, and P. C. F. Eggers, "Time Reversal in Wireless Communications: A Measurement-Based Investigation," *IEEE Transactions on Wireless Communications*, **5**, 8, November, 2006, pp. 2242-2252.
25. H. T. Nguyen, "On the Performance of One Bit Time Reversal for Multi-user Wireless Communications," 4th International Symposium on Wireless Communications Systems, October, 2007, pp. 672-676.
26. P. Blomgren, P. Kyritsi, A. D. Kim, and G. Papanicolaou, "Spatial Focusing and Intersymbol Interference in Multiple-Input – Single-Output Time Reversal Communication Systems," *IEEE Journal of Oceanic Engineering*, **33**, 3, 2008, pp. 341-355.
27. H. El-Sallabi, P. Kyritsi, A. Paulraj, and G. Papanicolaou, "Experimental Investigation on Time Reversal Precoding for Space-Time Focusing in Wireless Communications," *IEEE Transactions on Instrumentation and Measurements*, **59**, 6, June, 2010, pp. 1537-1543.
28. B. Wang, Y. Wu, F. Han, Y. Yang, and K. J. Ray Liu, "Green Wireless Communications: A Time-Reversal Paradigm," *IEEE Journal on Selected Areas in Communications*, **29**, 8, September, 2011, pp. 1698-1710.
29. F. Monsef, A. Cozza, and L. Abboud, "Effectiveness of Time-Reversal Technique for UWB Wireless Communications in Standard Indoor Environments," ICECom, Croatia, 2010.
30. A. Cozza, "Increasing Peak-Field Generation Efficiency of Reverberation Chamber," *Electronics Letters*, **46**, 1, January, 2010.
31. A. Cozza, and H. Moussa, "Enforcing Deterministic Polarization in a Reverberating Environment," *Electronics Letters*, **45**, 25, December, 2009.
32. H. Moussa, A. Cozza, and M. Cauterman, "Experimental Analysis of the Performance of a Time-Reversal Electromagnetic Chamber," Asia-Pacific International Symposium on Electromagnetic Compatibility, Beijing, China, 2010, pp. 1006-1009.
33. Andrea Cozza, "Statistics of the Performance of Time Reversal in a Lossy Reverberating Medium" *Physical Review*, **E 80**, 2009, p. 056604.
34. H. Moussa, A. Cozza, and M. Cauterman, "Directive Wavefronts Inside a Time Reversal Electromagnetic Chamber," *IEEE International symposium on Electromagnetic Compatibility*, 2009, pp. 159-164.
35. H. Saghir, M. Heddebaut, F. Elbahhar, A. Rivenq, and J. M. Rouvaen, "Time-Reversal UWB Wireless Communication-Based Train Control in Tunnel," *Journal of Communications*, **4**, 4, May, 2009, pp. 248-256.
36. V. Chatelee, A. Dubois, I. Aliferis, J.-Y. Dauvignac, C. Pichot and M. Yedlin, "Real Data Microwave Imaging and Time Reversal," IEEE International Symposium on Antennas and Propagation, June, 2007.
37. D. B. Battikh, J. Kelif, F. Abi Abdallah, and D. Phan-Huy, "Time Reversal Outage Probability for Wideband Indoor Wireless Communications," IEEE 21st International Symposium on Personal, Indoor and Mobile Radio Communications, September, 2010, pp. 999-1003.
38. A. Khalegi, "Measurement and Analysis of Ultra-Wideband Time Reversal for Indoor Propagation Channels," *Wireless Personal Communications*, **54**, 2, July, 2010, pp. 307-320.
39. F. Bellens, F. Quitin, J. Dricot, F. Horlin, A. Benlarbi-Delaï, P. De Doncker, "Performance Evaluation of Time Reversal in Intra-Vehicular Environment," Proceedings of the 5th European Conference on Antennas and Propagation, April, 2011, pp. 206-210.
40. P. Pajusco and P. Pagani, "On the Use of Uniform Circular Arrays for Characterizing UWB Time Reversal," *IEEE Transactions on Antennas and Propagation*, **AP-57**, 1, January, 2009, pp. 102-109.
41. J. M. F. Moura and Y. Jin, "Detection by Time Reversal: Single Antenna," *IEEE Transactions on Signal Processing*, **55**, 1, January, 2007, pp. 187-201.
42. Y. Jin, Y. Jiang, and J. M. F. Moura "Time Reversal Beamforming for Microwave Breast Cancer Detection," IEEE International Conference on Image Processing, ICIP 2007, September-October, 2007, pp. v-13-16.
43. P. Kosmas, E. Zastrow, S. C. Hagness, and B. D. Van Veen, "A Computational Study of Time Reversal Techniques for Ultra-Wideband Microwave Hyperthermia Treatment of Breast Cancer" IEEE/SP 14th Workshop on Statistical Signal Processing, SSP '07 , August, 2007, pp. 312-316.

44. P. Kosmas and C. M. Rappaport, "FDTD-Based Time Reversal for Microwave Breast Cancer Detection – Localization in Three Dimensions," *IEEE Transactions on Microwave Theory and Techniques*, **54**, 4, April, 2006, pp. 1921-1927.
45. P. Kosmas and C. M. Rappaport, "A Matched-Filter FDTD-Based Time Reversal Approach for Microwave Breast Cancer Detection," *IEEE Transactions on Antennas and Propagation*, **AP-54**, 4, April, 2006, pp. 1257-1264.
46. P. Kosmas and C. M. Rappaport, "Time Reversal with FDTD Method for Microwave Breast Cancer Detection," *IEEE Transactions on Microwave Theory and Techniques*, **53**, 7, July, 2005, pp. 2317-2323.
47. D. Liu, S. Vasudevan, J. Krolik, G. Bal, and L. Carin, "Electromagnetic Time-Reversal Source Localization in Changing Media: Experiment and Analysis," *IEEE Transactions on Antennas and Propagation*, **AP-55**, 2, February, 2007, pp. 344-354.
48. D. Liu, G. Kang, L. Li, Y. Chen, S. Vasudevan, W. Joines, Q. H. Liu, J. Krolik, and L. Carin, "Electromagnetic Time-Reversal Imaging of a Target in a Cluttered Environment," *IEEE Transactions on Antennas and Propagation*, **AP-53**, 9, September, 2005, pp. 3058-3066.
49. T. Liao, P. Hsieh, and F. Chen, "Subwavelength Target Detection using Ultrawideband Time-Reversal Techniques with a Multilayered Dielectric Slab," *IEEE Antennas and Wireless Propagation Letters*, **8**, 2009, pp. 835-838.
50. A. B. Ruffin, J. Whitaker, T. B. Norris, J. Decker, L. Sanchez-Palencia, LenGcLeHors, and J. V. Rudd, "Time Reversal and Object Reconstruction Using Single-Cycle Terahertz Pulses," *IEEE Lasers and Electro-Optics Society 13th Annual Meeting*, 2000, pp. 240-241.
51. G. S. Smith, "A Direct Derivation of a Single-Antenna Reciprocity Relation for the Time Domain," *IEEE Transactions on Antennas and Propagation*, **AP-52**, 6, June, 2004, pp. 1568-1577.
52. J. A. Kong, *Electromagnetic Wave Theory*, Cambridge, MA, EMW Publishing, 2005, pp. 703-704.
53. D. Ghosh, A. De, M. C. Taylor, T. K. Sarkar, M. C. Wicks, and E. L. Mokole, "Transmission and Reception by Ultra-Wideband (UWB) Antennas," *IEEE Antennas and Propagation Magazine*, **48**, 5, October, 2006, pp. 67-99.
54. L. Sevgi, "Reciprocity: Some Remarks from a Field Point of View," *IEEE Antennas and Propagation Magazine*, **52**, 2, April, 2010, pp. 205-210.
55. S. M. Narayana, G. Rao, R. Adve, T. K. Sarkar, V. C. Vannicola, M. C. Wicks, and S. A. Scott, "Interpolation/Extrapolation of Frequency Domain Responses Using the Hilbert Transform," *IEEE Transactions on Microwave Theory and Techniques*, **44**, 10, October, 1996, pp. 1621-1627.
56. B. Widrow and E. Walach, *Adaptive Inverse Control: A Signal Processing Approach, Reissue Edition*, Hoboken, NJ, John Wiley and Sons Inc., 2008.
57. M. C. Wicks, and T. K. Sarkar, "Century Bandwidth Antenna for Use in Applications with Waveform Diversity," *IEEE International Symposium on Antennas and Propagation*, July, 2008.
58. Audacity Team, "Audacity: The Free, Cross-Platform Sound Editor, Version 1.3.13-Beta," downloaded from <http://audacity.sourceforge.net/>, January, 2011.
59. J. S. Garofolo, L. F. Lamel, W. M. Fisher, J. G. Fiscus, D. S. Pallett, N. L. Dahlgren, and V. Zue, TIMIT acoustic-phonetic continuous speech corpus, Trustees of the University of Pennsylvania, 1993; downloaded from <http://www.ldc.upenn.edu/Catalog/CatalogEntry.jsp?catalogId=LDC93S1>.
60. M. Jeub, M. Schafer, and P. Vary, "A Binaural Room Impulse Response Database for the Evaluation of Dereverberation Algorithms," *Proceedings of International Conference on Digital Signal Processing (DSP)*, July, 2009.
61. R. F. Harrington, *Time-Harmonic Electromagnetic Fields*, New York, John-Wiley and Sons Inc., 1961.

Introducing the Feature Article Authors



Walid M. G. Dyab received the BSc and MSc from University of Alexandria, Alexandria, Egypt, in 2003 and 2007, respectively, both in Electrical Engineering. Currently, he is a doctoral candidate at Syracuse University, Syracuse, NY. From 2003 until 2005, he was a teaching assistant at the Alexandria Institute of Technology (AIT), Alexandria, Egypt. From 2005 until 2006, he worked as a Technical Support Engineer in the Radio Network Department at Alcatel, Egypt. From 2006

until 2009, he was a Teaching and Research Assistant at the German University in Cairo (GUC), Cairo, Egypt. His research interests include the fields of antennas and electromagnetic wave propagation, antenna measurements, adaptive antenna systems, and adaptive signal processing, design, and analysis of microwave passive circuits.



Tapan K. Sarkar received the BTech from the Indian Institute of Technology, Kharagpur, in 1969; the MScE from the University of New Brunswick, Fredericton, NB, Canada, in 1971; and the MS and PhD from Syracuse University, Syracuse, NY, in 1975.

From 1975 to 1976, he was with the TACO Division of the General Instruments Corporation. He was with the Rochester Institute of Technology, Rochester, NY, from 1976 to 1985. He was a Research Fellow at the Gordon McKay Laboratory, Harvard University, Cambridge, MA, from 1977 to 1978. He is now a Professor in the Department of Electrical and Computer Engineering, Syracuse University. His current research interests deal with numerical solutions of operator equations arising in electromagnetics and signal processing, with application to system design. He obtained one of the “best solution” awards in May 1977 at the Rome Air Development Center (RADC) Spectral Estimation Workshop. He received the Best Paper Award of the *IEEE Transactions on Electromagnetic Compatibility* in 1979, and at the 1997 National Radar Conference. He has authored or coauthored more than 300 journal articles and numerous conference papers, 32 chapters in books, and fifteen books, including his most recent books, *Physics of Multi-Antenna Systems and Broadband Adaptive Processing* (John Wiley & Sons, 2008); *Parallel Solution of Integral Equation-Based EM Problems in the Frequency Domain* (John Wiley & Sons, 2009); *Time and Frequency Domain Solutions of EM Problems Using Integral Equations and a Hybrid Methodology* (IEEE Press and John Wiley & Sons, 2010); and *Higher Order Basis Based Integral Equation Solver (HOBBIES)* (John Wiley & Sons 2012).

Dr. Sarkar is a Registered Professional Engineer in the State of New York. He received the College of Engineering Research Award in 1996 and the Chancellor’s Citation for

Excellence in Research in 1998 at Syracuse University. He was an Associate Editor for Feature Articles of the *IEEE Antennas and Propagation Society Newsletter* (1986-1988), Associate Editor for the *IEEE Transactions on Electromagnetic Compatibility* (1986-1989), Chair of the Inter-Commission Working Group of URSI on Time Domain Metrology (1990-1996), a Distinguished Lecturer for the Antennas and Propagation Society from 2000-2003, a member of the Antennas and Propagation Society AdCom (2004-2007), a member of the IEEE Electromagnetics Award Board (2004-2007), on the Board of Directors of ACES (2000-2006), Vice President of the Applied Computational Electromagnetics Society (ACES), Associate Editor for the *IEEE Transactions on Antennas and Propagation* (2004-2010), and on the editorial boards of *Digital Signal Processing – A Review Journal* and *Journal of Electromagnetic Waves and Applications* (2006-2012). He is an Associate Editor for *Microwave and Optical Technology Letters* and the 2013 President Elect for the IEEE Antennas and Propagation Society. He is a member of Sigma Xi and USNCI-URSI Commissions A and B. He received the Docteur Honoris Causa from the Université Blaise Pascal, Clermont Ferrand, France, in 1998; from the Polytechnic University of Madrid, Madrid, Spain, in 2004; and from Aalto University, Helsinki, Finland (2012). He received the Medal of the Friend of the City of Clermont Ferrand, France, in 2000.



Alejandro García-Lampérez was born in Madrid, Spain, in 1976. He received the MS and PhD in Telecommunication Engineering from the Polytechnic University of Madrid, Spain, in 2000 and 2004, respectively. From 1999 to 2007, he was with the Microwaves and Radar Group, Department of Signals, Systems and Radiocommunications, ETSI Telecomunicación, Polytechnic University of Madrid, Spain. In 2007, he joined the Radiofrequency Group, now Radiofrequency, Electromagnetics, Microwaves and Antennas Research Group, of the Department of Signal Theory and Communications, College of Engineering, Universidad Carlos III de Madrid (UC3M), Spain, where he is currently a Visiting Professor. Among his interests are the application of numerical and algebraic methods to modeling and simulation problems at high frequencies, and the synthesis and design of microwave and millimeter-wave passive devices and active filters.



Magdalena Salazar-Palma was born in Granada, Spain. She received the MS and PhD in Electrical and Electronic Engineering from Polytechnic University of Madrid, Spain, where she has been an Assistant Professor and an Associate Professor in the Department of Signals, Systems and Radio-communications. Since 2004, she has been with the Department of Signal Theory and Communications, Charles the Third University of Madrid, Spain, where she is a full Professor, co-Director of the Radiofrequency, Electromagnetics, Microwaves and Antennas Research Group (GREMA), and has served for three years as Head of the Department.

She has developed her research in a number of areas: electromagnetic field theory; advanced computational and numerical methods for microwave and millimeter-wave passive components and antennas analysis and design; advanced network and filter theory and design; antenna arrays and smart antennas; novel materials and metamaterials for the implementation of devices and antennas with improved performance (multi-band, miniaturization, and so on) for the new generation of communication systems; design, simulation, optimization, implementation, and measurement of microwave circuits, both in waveguide and integrated (hybrid and monolithic) technologies; millimeter and sub-millimeter frequency band technologies; and the history of telecommunications.

She has authored 610 scientific publications: seven books and 25 contributions for books published by international editorial companies; 13 contributions for academic books; 86 papers in scientific journals; 312 papers in international conferences, symposia, and workshops; 76 papers in national conferences; 53 project reports; 30 short course notes; and eight other publications. She has coauthored two European and USA patents, and several software packages for the analysis and design of microwave and millimeter-wave passive components, antennas, and antenna arrays, advanced filters and multiplexers for space applications, which are used by multi-national companies. She has participated (as principal investigator or researcher) in 88 research projects and contracts financed by international, European, and national institutions and companies. She has delivered numerous invited presentations and short courses. She received two research awards and other recognitions.

She was a member of the Spain Accreditation Committee of Full Professors in Engineering and Architecture and other accreditation panels for institutions in Spain and abroad. She has assisted several Spanish agencies in the evaluation of projects, research grant applications, and so on. She has served on

evaluation panels of the Commission of the European Communities, and various other countries, including the National Science Foundation in the USA. She has been a member of the editorial board or an associate editor of several scientific journals, a member of the technical program or organizing committee of many international and national symposia, and a reviewer for many international scientific journals, symposia, and editorial companies.

Since 1989, she has served the IEEE in different volunteer positions: Vice Chair and Chair of the Spain Section AP-S/MTT-S Joint Chapter, Spain Section Chair, Spain Section Membership Development officer and Professional Development officer, Region 8 Committee member, Region 8 Nominations and Appointments Subcommittee member, Chair of Region 8 Conference Coordination Subcommittee, Women in Engineering Committee (WIEC) member, Chair of WIEC, member of Ethics and Member Conduct Committee, History Committee, MGAB (Member and Geographic Activities Board) Geographic Unit Operations Support Committee, and elected member of AP-S Administrative Committee. She was elected 2010 AP-S President Elect, serving in 2011 as AP-S President and member of the Technical Activities Board (TAB), and, in 2012, as AP-S Past President and Chair of AP-S Nominations Committee. Currently, she is a member of the AP-S Administrative Committee as Past President, a member of the AP-S Distinguished Lecturer Program Committee, MTT-S Subcommittee #15, MTT-S Education Committee, Division IV Nominations and Appointments Committee, Service Awards Committee, and TAB Society Review Committee. She is the Chair of the AP-S History Committee and Sections Congress 2014 Committee.



Miguel Angel Lagunas was born in Madrid, Spain, in 1951. He received the Telecommunications Engineer degree in 1973 from UPM, Madrid, and the PhD in Telecommunications from UPB, Barcelona. During 1971-1973, he was a Research Assistant at the Semiconductor Lab ETSIT, Madrid. He joined UPC as Teacher Assistant in Network Synthesis and Semiconductor Electronics (1973-1979), and Associate Professor of digital signal processing (1979-1982). Since 1983, he has been a full Professor at UPC, teaching courses in signal processing, array processing, and digital communications. He was Project Leader of high-speed SCMA (1987-1989) and ATM (1994-1995) cable network. He is also co-Director of the first projects for the European Spatial Agency and the European Union, providing engineering demonstration models on smart antennas for satellite communications using DS and FH systems (1986) and antenna arrays for mobile communica-

cations GSM (1997). His research activity is devoted to spectral estimation, DSP on communications and array processing. His technical activities are in advanced front-ends for digital communications, combining spatial with frequency-time and coding diversity. Prof. Lagunas was Vice President for Research of UPC from 1986-1989, and Vice Secretary General for Research, CICYT, Spain, from 1995-1996. He was a member of the NATO scientific committee (1997-2001). Currently, he is Director of the Telecommunications Technological Center of Catalonia (CTTC) in Barcelona, and Secretary of the Spanish committee for large research facilities. He is an elected member of the Academy of Engineers of Spain, and of the Academy of Science and Art of Barcelona. He was a Fulbright scholar at the University of Boulder, CO. (✉)